ISTANBUL TECHNICAL UNIVERSITY ★ GRADUATE SCHOOL OF SCIENCE ENGINEERING AND TECHNOLOGY

EFFECT OF POTENTIAL CO-CHAPERONE MZB1 ON CHAPERONE GRP94

M.Sc. THESIS

Mustafa Barbaros DÜZGÜN

Department of Molecular Biology-Genetics and Biotechnology

Molecular Biology-Genetics and Biotechnology Programme

OCTOBER 2015

ISTANBUL TECHNICAL UNIVERSITY ★ GRADUATE SCHOOL OF SCIENCE ENGINEERING AND TECHNOLOGY

EFFECT OF POTENTIAL CO-CHAPERONE MZB1 ON CHAPERONE GRP94

M.Sc. THESIS

Mustafa Barbaros DÜZGÜN
(521121145)

Department of Molecular Biology-Genetics and Biotechnology

Molecular Biology-Genetics and Biotechnology Programme

Thesis Advisor: Assoc. Prof. Dr. Nevin GÜL KARAGÜLER

OCTOBER 2015

İSTANBUL TEKNİK ÜNİVERSİTESİ ★ FEN BİLİMLERİ ENSTİTÜSÜ

OLASI KOŞAPERON MZB1 PROTEİNİNİN GRP94 ŞAPERONU ÜZERİNDEKİ ETKİSİ

YÜKSEK LİSANS TEZİ

Mustafa Barbaros DÜZGÜN
(521121145)

Moleküler Biyoloji, Genetik ve Biyoteknoloji Anabilim Dalı

Moleküler Biyoloji, Genetik ve Biyoteknoloji Programı

Tez Danışmanı: Doç. Dr. Nevin GÜL KARAGÜLER

EKİM 2015

Mustafa Barbaros DÜZGÜN, a **M.Sc.** student of ITU **Graduate School of Science Engineering and Technology** student ID **521121145**, successfully defended the **thesis** entitled "**EFFECT OF POTENTIAL CO-CHAPERONE MZB1 ON CHAPERONE GRP94**", which he prepared after fulfilling the requirements specified in the associated legislations, before the jury whose signatures are below.

Thesis Advisor :	**Assoc. Prof. Dr. Nevin GÜL KARAGÜLER** İstanbul Technical University	….....
Jury Members :	**Prof. Dr. Ayten YAZGAN KARATAŞ** Istanbul Technical University	….....
	Assist. Prof. Dr. Emel ORDU Yıldız Technical University	.....

Date of Submission: 16 September 2015
Date of Defense : 05 October 2015

To my family,

FOREWORD

After passing an interesting year with outcome of acquired strong experiences but less harvest of experimental data than expected before starting this journey at TUM, I would like to point out my gratitude to my supervisor at ITU. I thank Prof. Nevin GÜL KARAGÜLER with my all sincere due to supporting me during my exchange studentship and the time span of that I was at ITU. Prof. KARAGÜLER has never hesitated to show her trust to me. Her advices made me pull myself together, especially in troubled times of the master thesis project.

I was very fortunate to get a chance to study under the laboratory of Prof. Johannes BUCHNER. Surely, his laboratory group is much more than moderate and it was great experience to be part of gear of his lab. The most significant aid of his lab group to me was to conceive the meaning of 'being productive'. Certainly, this is something effective, which would be required in academic life. It is my pleasure to thank Prof. BUCHNER for accepting me to his laboratory group and his support during duration of my stay.

I was very lucky to meet an esteemed scientist who is working under TUM family, Prof. Sevil WEINKAUF. She encouraged me to proceed in my thesis and to talk to her was a source of motivation. Her suggestions and statements regarding how to do science were rather valuable to me.

I would like to indicate my special thanks to Rahmi IMAMOĞLU. It was great coincidence to be in same city after sharing the same laboratory in Istanbul. This case let us keep our fruitful discussion on scientific topics.

I must emphasize my special thanks to Gökhan GÜN, Duygu KAVADARLI, Mevlüt ARSLAN, Varol GÜLER, Khaled ABU ALI, Nina PROKOPH, Hasan DEMİRCİ, Soner TORUN.

October 2015

Mustafa Barbaros DÜZGÜN
(Molecular Biologist)

TABLE OF CONTENTS

Page

ABBREVIATIONS

ADP : Adenosine diphosphate
AMP-PNP : Adenosine 5′-(β,γ-imido)triphosphate
ATP : Adenosine triphosphate
ATP- γS : Adenosine 5′-[γ-thio]triphosphate
CD : Circular dichroism
CS : Citrate synthase
EC_{50} : Half Maximal Effective Concentration
EM : Electron Microscopy
Grp94 : Glucose-regulated Protein 94
HEPES : 4-(2-hydroxyethyl)-1-piperazineethanesulfonic acid
H_2O : Water
Hsp : Heat Shock Protein
IMAC : Immobilized-Metal Affinity Chromatography
IPTG : Isopropyl β-D-1-thiogalactopyranoside
ITC : Isothermal Titration Calorimetry
KCl : Potassium chloride
LDH : Lactate dehydrogenase
$MgCl_2$: Magnesium chloride
NADH : Nicotinamide adenine dinucleotide
NBD : Nucleotide Binding Domain
NMR : Nuclear Magnetic Resonance
PAGE : Polyacrylamide gel electrophoresis
PDB ID : Protein Data Bank identification code
PMSF : Phenylmethanesulfonyl fluoride
PEP : Phospho(enol)pyruvic acid
P_i : Inorganic phosphate
PK : Pyruvate kinase
SAXS : Small-Angle X-ray Scattering
SLIC : Sequence- and Ligation-independent Cloning
SBD : Substrate Binding Domain
SDS : Sodium dodecyl sulfate
TRX : Thioredoxin
UV : Ultraviolet
wt : Wild-type

LIST OF TABLES

Page

LIST OF FIGURES

Page

EFFECT OF POTENTIAL COCHAPERONE MZB1 ON GRP94

SUMMARY

Grp94 is Hsp90 paralog, residing in endoplasmic reticulum (ER), implicated in efficient expression of various proteins secreted and presented on cell membrane. As an essential eukaryotic chaperone, a set of studies have already shown that Grp94 involves in maturation of Toll-like receptors, integrin family members and antibody secretion. Since the condition of ER significantly differs from that of the cytosol, Grp94 must have been uniquely evolved from its cytosolic counterparts in order to deal with distinct client profile of ER. It is known that vast majority of Grp94 clients possess at least one disulphide bond whose formation is crucial to attain 3-D structure and stability for many ER proteins. Besides, ER is much more oxidizing than cytosol due to its enzymatic components catalysing disulphide formation. Despite of having same domain organisation with those of other Hsp90 family members, in which N terminal domain preceding M domain and finally C-terminal domain functioning in dimerization, Grp94 has significant conformational differences compared to its cytosolic counterparts. Most importantly, unlike other Hsp90, in the presence of AMP-PNP or ADP, Grp94 adopts same twisted V conformation which seems to make N-terminal dimerization unfavourable. It must be noted that binding of ATP makes Hsp90 family members undergo some conformational changes in which N- terminal domains of each protomer dimerize resulting in ATP hydrolysis. Furthermore, unlike its cytosolic counterparts, Grp94 does not show different affinity profile for ATP and ADP. These data has been leading an intriguing question regarding to the extent in which Grp94 differs from its cytosolic homologs in undergoing conformational changes during its ATPase cycle. It is long standing enigma as to whether Grp94 is regulated by a co-chaperone which may mediate client loading or remodel ATPase cycle to function in maturation of a set of ER proteins. Even though some studies have shown that a set of protein interact Grp94 along with clues concerning physiological relevance, our current understanding of the precise nature of interaction in these presumptive proteins with Grp94 and their regulatory effects on Grp94 conformational changes are still infant. pERp1/MZB1 is relatively newly discovered protein residing in ER. Its function has not been fully understood, which presumably act as an unique oxidoreductase or chaperone. In previous studies, it has been demonstrated that pERp1 interacts with ER chaperones, Grp94 and BiP. In the context of this thesis, wild type Grp94 and a flanked at both terminal domains by partial ubiquitin version of Grp94 are compared by subjecting to ATPase assay and circular dichroism spectroscopy. The main aim is to check whether ubiquitin tagged Grp94 has no significant difference from wild type in ATPase kinetics and secondary structure. It must be noted that this version was important to do further investigation on Grp94 by single molecule study. Moreover, titration of pERp1 has been performed to calculate EC_{50} which is an indicator of binding affinity. Apart from steady state kinetics, citrate synthase aggregation assay and analytical size exclusion chromatography are applied to the respective proteins.

.

OLASI KOŞAPERON MZB1 PROTEİNİNİN GRP94 ŞAPERONU ÜZERİNDEKİ ETKİSİ

ÖZET

Glükoz regüle protein 94 (Grp94) ısı şok protein ailesinin üyesi olan Hsp90'ın endoplasmik retikulum (ER) paraloğudur. Birçok çalışmada Grp94 sekresyona uğrayan veya hücre membranında fonksiyon gösteren çeşitli proteinlerin efektif ekspresyonu ile ilişkilendirilmiştir. Grp94 ökaryotik hücreler için elzem bir şaperondur ve üzerine yapılan bazı fonksiyonel çalışmalar Grp94'ün Toll-like reseptörü, integrin ailesi gibi bazı proteinlerin son yapılarının kazanmasında ve antikor sekresyonunda rol aldığını göstermiştir. Endoplasmik retikulum organelinin protein içerik ve katlanma profili hücre sitozolüne oranla çok büyük farklılıklar göstermesi Grp94'ün farklı özellikler kazanarak evrimleşmiş olabileceğinin en önemli göstergesidir. Bu özellikler Grp94'ün otantik ER proteinlerin katlanma sürecinde rol oynamasını evrimsel süreç içerisinde önünü açmış olabilir. Örneğin, Grp94'ün müşteri proteinlerin dikkate değer en önemli farklılığı disülfid bağ(lar) içermeliridir.

Hsp90 ailesindeki tüm homologlar aynı domain organizasyonuna sahiptir; sırasıyla N-terminal domain, orta domain (M) ve C-terminal domaindir. Grp94 de aynı domain sıralamasına sahip olmasına rağmen, kendine özgü konformasyona adapte olmuştur. Bu konformasyon literatürde 'Kıvrılmış V Konformasyonu' olarak adlandırılmış olup Hsp90 konformasyonunda katalitik aktivite ile ilişkilendirilmiş 'N-terminal domain dimerleşmesini' mümkün kılmayacak niteliktedir. Nükleotid regüle olan Hsp90 ailesi ATP'nin bağlanmasıyla N-terminal domain dimerizasyonu ile başlayan büyük konformasyonal değişikliklere uğrar ve ardaşık konformasyonlar ATP'nin hidrolizi ve ADP'nin salınmasıyla sona erer. Bu veriler Grp94'ün ATPaz deviri sırasında hangi seviyede tanımlanan konformasyonlara adapte olduğunun irdelenmesine sebep olmaktadır. Grp94'ün 'Kıvrılmış V Konformasyonu' ATP aktivitesi için uygun olmamakla beraber, kristal yapısı (AMP-PNP ya da ADP) nükleotid kimliği ile değişmemiştir.

Hsp90 şaperon protein ailesinin ATP ile tetiklenen konformasyonel deviri ATP'nin N-terminal domainde yer alan nükleotid bağlanma oyuğuna yerleşmesiyle başlar. Kapak görevi gören N-terminal yapı birimi ATP'nin üzerini kapatacak şekilde pozisyonlanması ile iki protomerin N-terminal domainleri dimerleşmesi tetiklenir. Bu konformasyonun dimerizasyonu daha sonra M domainin N-terminal domain ile temas kurmasına sebep olur ve ATP'nin kimyasal parçalanması vuku bulur. Daha sonra ADP ve P_i N-terminal domaini terk eder. Böylelikle Hsp90 tekrar yeni bir ATPaz devirine başlamaya hazır başlangıç konformasyonuna tekrar adapte olur. Grp94'ü diğer sitozolik Hsp90 üyelerinden ayıran bir diğer özelliği ATP'ye ve ADP'ye bağlanma eğiliminin aynı seviyede olmasıdır. Hem konformasyonel hem de bağlanma eğilimi açısından Grp94'ün ATP ve ADP'ye karşı profilinin değişmemesi

Grp94'ün ATPaz devirisi sırasında hangi düzeyde sitozolik Hsp90 üyelerinden farklılık gösterdiği sorusunun sorulmasına sepeb olmaktadır.

Grp94'ün herhangi bir koşaperonun yardımı ile ATPaz devirinin regüle edilip edilmediği veya müşteri proteinleri ile etkileşime girmesinin sağlanıp sağlanmadığı uzun süren bir muammadır. Ayrıca, Grp94'ün birtakım potansiyel koşaperonlar ile etkileşime girdiği ve fizyolojik önemi açısından literatür bilgisi olmasına rağmen, müşteri proteinlerinin olgunlaşmasındaki fonksiyonu ve bu etkileşimin yapısal-mekaniksel altyapısı hakkında herhangi bir ipucu şu ana kadar literatürde belirtilmemiştir. Potansiyel koşaperonların Grp94 üzerindeki etkisini araştıran üzerine şu anda kısıtlı bilgiler mevcuttur.

Bu tezde potansiyel koşaperon olarak düşündüğümüz pERp/MZB1 proteini kararlı hal kinetiği deneylerinde kullanılarak Grp94'ün ATPaz aktivitesine etkisi araştırılmışır. pERp1 nispeten yeni keşfedilmiş bir endoplazmik retikulum proteini olup hücre içindeki fonksiyonu tam olarak bilinmemektedir. Literatürdeki çalışmalar pERp1'in büyük olasılıkla özgün bir oksidoredüktaz ya da şaperon olduğunu ileri sürmektedir. Üzerine yapılan çalışmalardan bazıları pERp1'in BiP (Hsp70'in ER paraloğu) ve Grp94 gibi endoplazmik retikulum şaperolarıyla etkileşiğini ortaya koymuştur. Ek olarak, önceki çalışmalar pERp1'in immünoglobin katlanmasında, hafif zincirlerin takımlaşmasında ve sekrasyonunda rol aldığını göstermiştir.

Tez kapsamında, yabanıl tip Grp94 ve hem N-terminal hem de C-terminal domain uçlarında kırpılmış ubikuitin eklenmiş, manipüle tip Grp94 (Ubi-Grp94-Ubi) ATPaz ve dairesel dikroizm spektroskopi deneyleri ile karşılaştırılmıştır. Bu deneylerdeki asıl amaç yabanıl ile manipüle edilmiş tip arasında kaydadeğer kinetik ve yapısal farklılıkların ortaya konmasıdır. Zira manipüle tipin (Ubi-Grp94-Ubi) klonlanmasının altında yatan sebep, yabanıl tipin içeriğinde bulunan 3 sistein amino asit molekülünün 'tek molekül çalışmasında' kullanılan, ticari florofor boyası Atto 488 ile kimyasal tepkimeye girmemesidir. Kırpılmış ubikuitin proteinin kimyasal olarak tepkimeye girebilecek, yapısal anlamda açıkta 1 sisteini bulunmaktadır. Ayrıca, potansyel koşaperon pERp1 ATPaz deneylerine eklenerek Grp94 üzerindeki kinetik etkisi araştırılmıştır. Kararlı hal kinetiği çalışmaları içerisinde farklı pERp1 konsantrasyonları Grp94'ün ATPaz aktivite deneylerine uygulanarak 'Etkili Konsantrasyon (EK_{50})' hesaplanmıştır. Hesaplanan EK_{50} değeri pERp1 Grp94 arasındaki bağlanma eğilimi hakkında ilk bilgiyi ortaya koymuştur. Bu deneylerle pERp1'ın Grp94 ATPaz aktivitesini önemli ölçüde arttırdığı gösterilmiştir. Ek olarak, Ubi-Grp94-Ubi versiyonunun ATP'ye bağlanma eğilimi K_m hesabıyla ortaya konulmuş ve literatürde önceden belirlenen yabanıl tip K_m'si ile karşılaştırılmıştır. Deney sonucu manipüle tip Grp94'ün ATP'ye olan bağlanma eğiliminde düşüklük saptanmıştır.

Şaperon proteinler normal büyüme koşullarında protein katlanmasını katalizlemesi yanı sıra termal stress gibi sert koşullarda hücre içerisinde proteinlerin yanlış katlanmasını ve kümeleşmesini önlemektedir. Hsp90 ailesi kendi müşteri proteinlerinin son olgunlaşma evresinde rol oynamaktadır ancak birçok şaperon ailesi gibi sert koşullar altında müşterisi olmayan proteinlerin stabilizasyonunda da rol almaktadır. Tez kapsamında, pERp1 ve Ubi-Grp94-Ubi proteinlerinin kümeleşmeye olan etkisi model protein sitrat sentaz kullanımıyla gerçekleştirilmiştir. Sitrat sentaz mitokondri matriksinde bulunan yüksek ısı koşullarında kümeleşmeye eğilimli bir enzimdir ve kümeleşme düzeyi spektroskopik yöntemlerle kolaylıkla takip edilebildiği için şaperon proteinlerin fonksiyonel çalışmaları için uygun bir modeldir.

Kinetik deneylere ek olarak, bu deney pERp1'in jenerik bir şaperon olmadığını aksine kümeleşmeyi hızlandırdığı ancak manipüle tip Grp94' ün fonksiyonel anlamda etkin olduğunu göstermiştir.

Önceki çalışmalar, pERp1 ve Grp94 etkileşiminin immünoglobin biyosentezi için önem taşıdığını ortaya koymuştur. Bu çalışmalarda Grp94-pERp1 etkilişimi ko-immünopresipitasyon deneyleri ile açıklığa kavuşturulmuştur. Tez kapsamında, bu etkileşimin bir başka yöntem olan analitik jel filtrasyon deneyleri ile validasyonu amaçlanmıştır. Ayrıca bu teknik pERp1 proteininin oligomerizasyon karakterinin belirlenmesinde fikir vermiştir.

Tez içeriği Grp94'ün olası bir koşaperon ile yapısal ve mekaniksel yaklaşımlar içeren bir projenin başlangıç aşaması niteliğindedir. Tez kapsamında önemli kinetik verilere erişilmiş olup pERp1'in Grp94 ATPaz devirinde etkili bir ajan olduğu saptanmıştır. Bu veriler çerçevesinde pERp1'in Grp94 konformasyonu üzerine genel senaryolar tartışma kısmında açıklanmaştır. Temel soruları açıklığa kavuşturacak etkileşimin yapısal analizi ve tek molekül çalışmaları Grp94 koşaperon muammasında temel tekniklerdir.

1. INTRODUCTION

1.1 Protein Folding and Molecular Chaperones

Protein folding is the process by which polypeptide sequences attain their unique 3-D structure. In the cellular environment, the adopted structures are required for the plethora of functions that proteins exert in the living cell. In 1972, Christian Anfinsen was awarded the Nobel Prize for discovering that protein folding is a spontaneous process which relies on the primary sequence of the polypeptide chain. The study was based on *in vitro* experiments which revealed that purified Ribonuclease A is refolded spontaneously without any additional factor assisting this process (Anfinsen, 1973). Attributed to this milestone discover, early on, it was thought that after the translation of a polypeptide, intramolecular interactions were sufficient to shape the unique 3-D structure. However, later, it was realised that, in many cases, protein folding in living organisms involves additional molecular machines which assist the folding process. These cellular components are called molecular chaperones and present a fundamental branch of the protein quality control network. Proteome integrity and proteostasis strictly depends on the chaperone network. In principle, chaperones function in preventing undesired intramolecular and intermolecular interactions, which result in misfolded states. Basically, chaperones ensure efficient protein folding in the cell.

1.2 *In Vivo* Protein Folding and Chaperone Protein Concept

In order to understand how the *in vivo* protein folding process differs from *in vitro* protein folding, the discrepancy between the conditions in the cellular environment and the test-tube must be taken into consideration. Most importantly, the cytosol contains high protein content with protein concentrations reaching up to 300 mg/ml in *E. coli* (Zimmerman & Trach, 1991). Compared to the test tube, the cytosol is a highly crowded milieu in which the folding process is dramatically influenced by macromolecular crowding. This is associated with an excluded volume effect and disturbs the entropic freedom of folding polypeptides (Ellis & Minton, 2006). As a

result of the excluded volume effect, the intermolecular affinity constants are influenced, which enhances the susceptibility of cellular aggregation (Zimmerman & Minton, 1993). Moreover, the protein translation process increases the risk of misfolding and aggregation due to the emerging nascent polypeptide chain which is not acquired fully folded conformation. Proteins emerging from the exit channel of the ribosome need to either have been translated completely or at least as single domain in order to be folded to the native state (Deuerling & Bukau, 2004). In structural aspect, the ribosome exit channel is approximately 100 Å in length, but the diameter only allows a polypeptide to attain alpha-helix secondary structures. Thus, the emerging nascent chain is exposed to the crowded cytosol before folding process is completed by which polypeptide is stabilized by its native state (Ban et al., 2000; Lu & Deutsch, 2005). The emerging nascent chain can adopt partially folded states and can become engaged in undesired intramolecular interactions. In such cases, propogation of misfolded state or even toxic aggregates can occur, consequently leading to a metabolic burden for cell. To combat challenges of both co-translational and post-translational protein folding, living organisms have developed a diverse set of structurally unrelated molecular chaperones which assist cellular polypeptides to acquire their unique 3-D structures. Importantly, many members of the chaperone network belong to the heat-shock class and are upregulated under stress conditions (Vabulas et al., 2010). Under harsh circumstances, polypeptides in the cell are threatened to lose their unique structure, which disturbs the cellular protein homeostasis. In this case, the protection of the stability of proteins is highly important since conformational equilibrium of protein contents may dramatically shifts to non-native states which may result in loss of catalytically active conformation and raise of aggregation-prone conformers (Vabulas et al., 2010). Once the stress-denatured protein species are upregulated with high temperature or oxidative stress, a set of cellular agents called as ‘Heat Shock Protein (Hsp)’ are induced to create a network triggering protection as members of protein quality control mechanism. Therefore, primarily safeguard proteins, chaperones mainly are members of heat shock or stress-induced protein families (Vabulas et al., 2010). The function and cellular regulation of the chaperone network is thus, under both physiological and stress conditions, in the centre of protein folding.

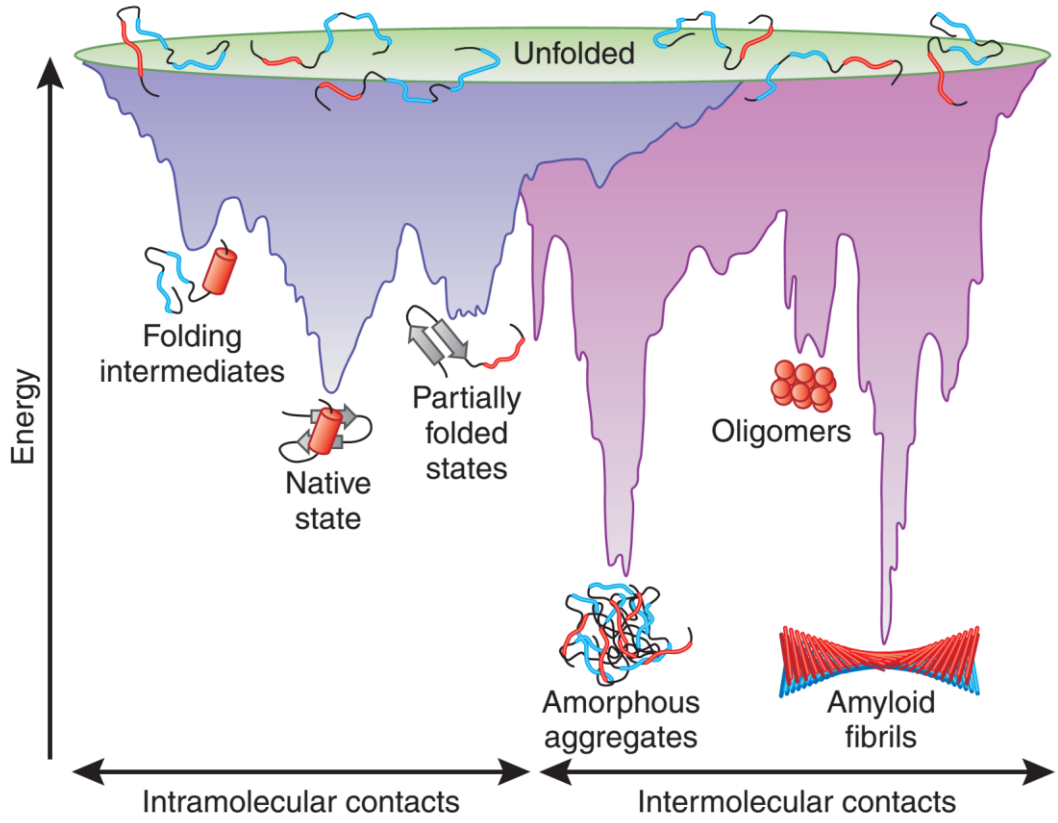

Figure 1.1 : Energy landscape representation of protein folding: The purple area represents the energy landscape of folding states originating from intramolecular interactions of a single polypeptide, such as partially folded states and the native state. The pink area depicts energy states of protein species arising from intermolecular interaction, in which possible states are amyloid fibrils, oligomers and amorphous aggregates (Hartl & Hayer-Hartl, 2009).

Molecular chaperone protein is defined as any protein which either interacts and assists non-native conformers to fold into native conformation, or stabilizes to prevent undesired interactions (Hartl & Hayer-Hartl, 2009). These fundamental elements function in many cellular events, particularly *de nova* protein folding, refolding and disaggregation of off-pathway conformers and aggregates, polypeptide translocation into cellular compartments (Hartl et al., 2011). Over the course of evolution, chaperones have adapted to basically recognize hydrophobic motifs to protect the proteome from off-pathway which is navigated by undesired intramolecular and intermolecular interaction, rather than having steric information correspond to structure of the client (Hartl & Hayer-Hartl, 2009). A set of essential proteins such as tubulin and actin have strenuous folding pathway, consequently shows high dependence on chaperone proteins to deal with the challenge of their

trajectories which favourably last with non-native conformation and toxic aggregation (Hartl & Hayer-Hartl, 2009).

Many structurally unrelated chaperone families serve as protectors of cellular protein integrity and homeostasis with their unique mode of actions (see table 1.1 and 1.2). Chaperones are mainly catagorized and named on basis of their molecular weights: small Hsp (sHsps), Hsp40, Hsp60, Hsp70, Hsp90 and Hsp100. Vast majority of chaperones are regulated by nucleotide, in which conformational cycle is associated with ATPase cycle. To illustrate, Hsp70 family is a ubiquitious chaperone machine which assists both co-translational and post-translational protein folding (Kim et al., 2013). It is highly conserved from eubacteria to eukaryotes, interacting with substates in their unfolded, misfolded and aggregated states. In structural aspect, Hsp70 consists of two domains which are connected by a conserved hydrophobic linker. Hsp70 family involves in allosteric mechanism between nucleotide-binding domain (NBD) and substrate-binding doman (SBD) in which ATP binding into NBD regulates substrate interaction by increasing dissociation constant with decreasing affinity, and substrate binding into hydrophobic pocket of SBD triggers ATP hyrolysis (Mayer, 2013). Subsequent conformational changes take place with binding of substrate and nucelotide identity. Up to now, two conformations of Hsp70 has been illuminated, referred as ‘closed conformation’ and ‘open conformation’ on basis of lid proximity in respect of beta sandwich of SBD (Bertelsen et al., 2009; Kityk et al., 2012). The identity of nucleotide regulates respective conformations: ADP-bound Hsp70 adopts ‘closed’ whereas ATP-bound does ‘open’ conformations. Addition to nucleotide regulated conformational flexibity of Hsp70, two co-chaperone families J-domain protein (JDPs) and nucleotide-exchange factor (NEFs), which function in synergism with Hsp70 increases the hydrolytic power of the Hsp70 by influencing energitical barrier between the two conformations. In basic, NEFs increases dissociation constant of ADP, JDPs transfer substrates to Hsp70 and regulate the ATPase activity (Mayer, 2013). In case of interaction with substrate, Hsp70 family binds a motif defined as 5 hydrophobic amino acids flanked by positively charged amino acids (Rudiger et al., 1997). What makes Hsp70 a versatile molecular chaperone is that the hydrophobic motif it interacts is present per 30-40 residues in almost any polypeptide of proteome. In the native conformation, this motif is positioned at the hydrophoic core and only exposed at the early stage of

Table 1.1 : Members of Hsp40, Hsp70 and Hsp90 (Chang et al., 2007).

	Kingdom	Organism	Chaperone/Protein Data Bank ID	Monomer (kDa)/ Oligomeric State	Cochaperone/Cofactor	Subcellular Localization/Activity
Hsp70 System	Eubacteria	*E. coli*	DnaK/1DKG; 1DKZ	69/monomer	DnaJ, GrpE, ClpB	Cytosol/folding of nascent proteins; export of some proteins; reactivates heat-inactivated proteins; facilitates abnormal protein degradation; works with ClpB in protein aggregate disassembly; regulates heat-shock response.
	Archaea	Methanosarcinae	DnaK	67/monomer	DnaJ, GrpE	Cytosol/similar to bacterial DnaK.
	Eukaryotes	*S. cerevisiae*	Ssa1-4	70/monomer	Ydj1, Sis1, Sti1, Snl1, Fes1, Sse1/2, Cns1	Cytosol/folding of newly synthesized proteins; protein transport into ER, mitochondria.
			Ssb1,2	66/monomer	Zuotin, Sse1/2, Ssz1	Cytosol/folding of ribosome-bound nascent chains.
			Pdr13p/Ssz1	58/heterodimer	Zuotin	Cytosol/Zuotin cofactor; modifies Zuotin-Ssb interaction; folding of nascent chains on ribosomes.
			Sse1/2	77/monomer; heterodimer	Ssa1, Ssb1, Sis1	Cytosol/nucleotide exchange factor for Ssa and Ssb Hsp70s; participates in protein folding and refolding.
		Mammals	Hsc70, Hsp70/1YUW	71/monomer	Hsp40, Hop, Bag1-5, Hip, HspBP1, CHIP, SGT, TPR1, Tom70, Hsp110 homologs	Cytosol/mediates nascent polypeptide folding; protein transport into ER, mitochondria, nucleus; promotes lysosomal degradation of cytosolic proteins; inhibits polyglutamine fibril formation.
			Hsp110	97/monomer	Hsp70	Cytosol/prevents protein aggregation under stress; similar to *S. cerevisiae* Sse1/2.
			Hsp70L1	55/heterodimer	MPP11	Cytosol/folding of nascent chains on ribosomes; similar to *S. cerevisiae* Ssz1.
		S. cerevisiae	Kar2	74/monomer	Sec63, Scj1, Jem1, Lhs1, Sil1/Sls1	ER/protein translocation into ER; binds to unassembled/misfolded ER protein subunits; regulates unfolded protein response.
			Lhs1	97	Kar2	ER/Hsp110 homolog; nucleotide exchange factor of Kar2.
		Mammals	Bip/Grp78	72/monomer	Grp170, Sil1/Sls1	ER/similar to Kar2; multimeric ER protein assembly.
		S. cerevisiae	Ssc1	71/monomer	Tim14, Tim16, Tim44, Mdj1, Mge1	Mitochondria/protein translocation and folding in mitochondria.
			Ssc3/Ecm10	70/monomer	Mge1	Mitochondria/assists some mitochondrial protein complex assembly; mediates folding of imported proteins?
			Ssq1	72/monomer	Jac1, Mge1	Mitochondria/protein complex assembly; Fe/S cluster insertion.
		Mammals	mtHsp70	74/monomer		Mitochondria/similar to *S. cerevisiae* Ssc1.
			ctHsp70	68/monomer		Chloroplast/folding of imported proteins; insertion of light-harvesting complex protein into thylakoid membrane.
Hsp40	Eubacteria	*E. coli*	DnaJ/1EXK	41/dimer	DnaK, GrpE	Cytosol/binds to and accelerates ATP hydrolysis by DnaK; recruits DnaK to nascent chains; recognizes hydrophobic peptide segments in unfolded proteins.
	Eukaryotes	*S. cerevisiae*	Ydj1,Sis1/1NLT	45, 38/dimer	Ssa	Cytosol/interacts with non-native polypeptides triggering ATP hydrolysis by Ssa; protein transport across membranes.
		Mammals	Hdj1 (Hsp40), Hdj2, Auxilin	39, 38, 100	Hsp70, Hip	Cytosol/regulation of Hsc70 ATPase cycle; efficient loading of peptide substrate onto Hsc70. Auxilin recruits Hsc70 to clathrin-coated vesicles and promotes vesicle uncoating.
		S. cerevisiae	Scj1	35	Kar2	ER lumen/regulates protein folding in ER lumen; acts as a J protein for Kar2.
			Sec63	75	Kar2	ER membrane/SRP-independent posttranslational translocation into ER; works with Sec61 complex and Kar2.
			Mdj1	49	Ssc1, Tim14, Tim 16	Mitochondria/mitochondrial biogenesis and folding of newly imported proteins.
Hsp90	Eubacteria	*E. coli*	HtpG/1Y4U; 1SF8	71/dimer		Cytosol/protein refolding in stressed cells.
	Eukaryotes	*S. cerevisiae*	Hsp82/2CGE; 1US7	81/dimer	Sti1, Aha1, cdc37, p23/Sba1, Ppt1, CPR6	Cytosol/folding and conformational regulation of signaling proteins; reactivation of stress-denatured proteins; a capacitor of phenotypic variation.
		Mammals	Hsp90 (Hsp83, Hsp89)	85/dimer	Hop, Hip, Hsp70, p50, p23, CHIP, Sgt1, TPR2, Immunophilins (Cyp40, FKBP38, FKBP51, FKBP52)	Cytosol/similar to *S. cerevisiae* homolog; folding and regulation of steroid hormone receptors and many kinases.
		A. thaliana	AtHsp90-1,2,3,4	81	Hop, Sgt1, Immunophilin	Cytosol/cytokinin signalling and plant development.
		Mammals	Grp94 (ERp99)	86/dimer	Grp78	ER/folding and assembly of some secretory proteins.
		A. thaliana	AtHsp90-7	94		ER/function unknown; similar to Grp94?
			AtHsp90-5	88		Chloroplast/unknown

potein folding or in denaturation conditions. The positional state of the motif in respect of folding process explains why Hsp70 interacts primarily with unfolded and misfolded proteins (Mayer, 2013).

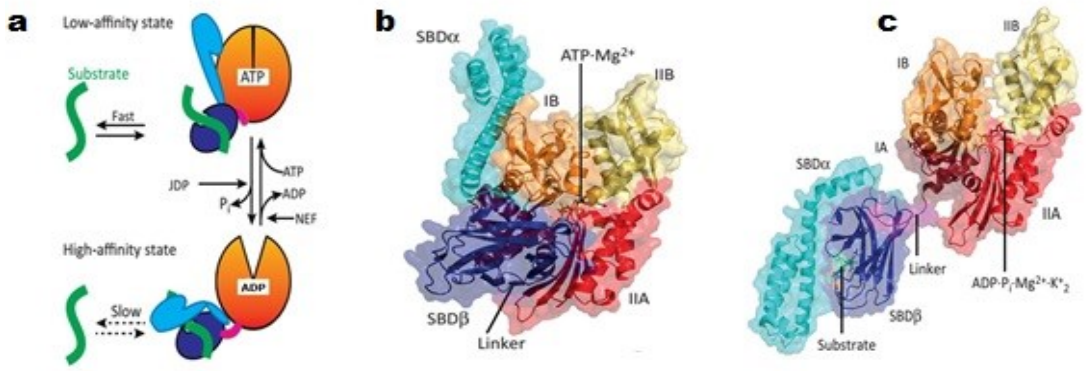

Figure 1.2 : Conformational change of Hsp70 and the cyrstal structures in respect of ATP and ADP (Mayer, 2013). a) Allosteric mechanism involves nucleotide-driven two conformations in which ATP-bound open conformation makes substrate association and dissociation favorable with low affinity whereas ADP-bound has high affinity that dramatically decreases substrate dissociation. Substrate binding triggers ATP hydrolysis which causes conformational changes transmitted to SBD domain, lasting with closure of lid over the beta sandwich. b) ATP-bound open conformation (PDB ID: 4B9Q). c) ADP-bound closed conformation (PDB ID: 2KHO).

In contrast to Hsp70, in structure, chaperonins are chamber-like large oligomeric, double- ringed complexes which are divided into two groups: Group I (Hsp60, GroEL, in eubacteria) and Group II (Thermosome in archea, TRİC/CCT in eukaryotes) (Tang et al., 2007). Group I consists of one pair of ring, of which each has seven subunits and the assembly cooperates with cap-like co-chaperone, Hsp10 whose structure is composed of one ring of seven subunits (GroES). Group II ring is made up of eight or nine subunits and lacks of Hsp10 counterpart (Hartl & Hayer-Hartl, 2009). One striking difference among the member of chaperonin family is that GroEL and the thermosome are in inducible character under heat stress whereas TRİC/CCT is not upregulated thermally (Horwich et al., 2007).

GroEL has been reported to interact more than 250 proteins, of that 85 are obligated substrates which contains TIM barrel fold (Kerner et al., 2005). The structural basis of the interactions with such wide-range clients depends on the hydrophobic groove around opening face of the cavity which exhibits plasticity facilitating optimized interaction platform in respect of different clients. Essentially, GroES serves as a lid for encapsulation in processing of the clients. GroES interaction with GroEL causes

Table 1.2 : Members of chaperonins, Hsp100, ribosome-associated chaperones and other chaperones (Tang et al., 2007).

		Kingdom	Organism	Chaperone/ Protein Data Bank ID	Monomer (kDa)/Oligomeric State	Cochaperone/Cofactor	Subcellular Localization/Activity
Ribosome-Associated Chaperones		Eubacteria	*E. coli*	Trigger factor/ 1W2B; 2AAR	48/dimer		Cytosol/assists folding of nascent chains; catalyzes peptidyl-prolyl isomerization in vitro.
		Eukaryotes	*S. cerevisiae*	NAC (α, β)	19, 17/heterodimer	SRP	Cytosol/interacts with ribosomes, SRP and translating polypeptide chains; role in protein folding/quality control?
				RAC (Ssz1, Zuotin)	58, 49/heterodimer	Ssb	Cytosol/interacts with Ssb; folding of nascent chains on ribosomes?
Chaperonins	Group I	Eubacteria	*E. coli*	GroEL/1AON	57/14mer	GroES	Cytosol/folding of a cytosolic protein subset; stabilizes proteins during heat stress; promotes folding in vivo of overproduced proteins; refolding of many proteins in vitro.
		Archaea	Methanosarcinae	GroEL	58/14mer	GroES	Cytosol/folding of cytosolic proteins; the only archaeal species that has GroEL.
		Eukaryotes	*S. cerevisiae*	Hsp60	~60/14mer	Hsp10	Mitochondria/folding of newly imported proteins; binds to heat-denatured mitochondrial proteins and prevents aggregation.
			Mammals	mtHsp60	~60/14mer	Hsp10	Mitochondria/folding of newly imported proteins.
			A. thaliana	Cpn60 (α and β)	57,58/Hetero 14mer	Cpn10, Cpn21	Chloroplast/folding and assembly of chloroplast proteins, e.g., ribulose bisphosphate carboxylase.
	Group II	Archaea	*T. acidophilum*	Thermosome (α and β)/1A6D	58/Hetero 16mer	Prefoldin/GimC	Cytosol/stress-inducible, promotes folding of a protein subset; refolding of unfolded polypeptides in vitro.
		Eukaryotes	*S. cerevisiae*/ Mammals	TRiC/CCT (α - θ)	57–60/Hetero 16mer	Prefoldin/GimC, PhLP	Cytosol/folding of a cytosolic protein subset, including actin, tubulins, and WD40 domain proteins; downstream of Hsp70 in de novo folding; assembly of polyglutamine expansion proteins into nontoxic oligomers.
Hsp100		Eubacteria	*E. coli*	ClpA	83/hexamer	ClpP, SspB	Cytosol/works with ClpP protease in ATP-dependent unfolding and proteolysis.
				ClpB/1QVR	96/hexamer	DnaK, DnaJ, GrpE	Cytosol/ATP-dependent protein disaggregation with DnaK.
		Eukaryotes	*S. cerevisiae*	Hsp104	104/hexamer	Hsp70, Hsp40	Cytosol/reactivates heat-damaged proteins; establishes and maintains the [PSI] yeast prion phenotype.
				Hsp78	85	Ssc1, Pim1	Mitochondria/prevents aggregation; degradation and turnover of unassembled mitochondrial proteins.
		Plants		ClpC	100	ClpP	Chloroplast/works with the ClpP protease to promote proteolysis.
Small Heat Shock Proteins (sHsp)		Eubacteria	*E. coli*	IbpA, IbpB	16/A: monomer; B: dimer/multimer		Cytosol/prevents heat-denatured protein aggregation; associates with inclusion bodies; works with DnaK in protein refolding.
		Archaea	*M. jannashii*	Hsp16.5/1SHS	16.5		Cytosol/stabilizes unfolded polypeptides and prevents aggregation.
		Eukaryotes	*S. cerevisiae*	Hsp26/2H50	24/24mer		Cytosol/prevention of protein aggregation; temperature-dependent dissociation required for efficient non-native substrate binding.
			Mammals	α-crystallin	32mer		Cytosol/in the vertebrate eye lens; prevents heat-denatured protein aggregation.
Other Chaperones		Eubacteria	*E. coli*	Hsp33/1VZY	33/dimer (active form)		Cytosol/redox-regulated molecular chaperone; prevents aggregation of thermally unfolded and oxidatively damaged proteins.
				SecB/1QYN	17/tetramer	SecA	Cytosol/stabilizes some secretory proteins in an unfolded state for export.
				Skp/1SG2	17/trimer		Periplasm/interacts with outer membrane proteins, maintains solubility of folding intermediates in the periplasm.
				PapD/3DPA	27/monomer	PapC	Periplasm/P Pili assembly in the chaperone-usher pathway.
				FimC/1BF8	23/monomer	FimD	Periplasm/Type 1 Pili assembly in the chaperone-usher pathway.
		Eukaryotes	Mammals	Calnexin/1JHN	90/monomer	ERp57, EDEM	ER membrane/works with glycosyltransferase to fold ER glycosylated proteins; interacts with some non-native proteins independent of glycosylation.
				Calreticulin	60/monomer	ERp57, EDEM	ER lumen/similar to calnexin.
				Hsp47	47	P4H	ER/binds to collagen; chaperone in the collagen biosynthetic pathway.

dramatic structural changes in the cavity by which the hydrophobic residues are replaced by polar ones, basically. Thereby, the binding affinity for client critically decreases, and the client is unleashed in the cavity (Walter & Buchner, 2002).

As in Hsp70 and Hsp90, GroEL is regulated by ATP binding and hydrolysis. The two rings asymmetrically function by which each is in different phases of cycle. There is positive cooperativity of ATP binding into each subunit (7 ATP per ring) for a ring. Conversely, between two rings negative cooperativity takes place, resulting in asymmetrical conformational changes in the ATPase cycle of the rings (Horwich et al., 2007). ATP-directed reaction cycle of GroEL-GroES complex is illustrated in Figure 1.3.

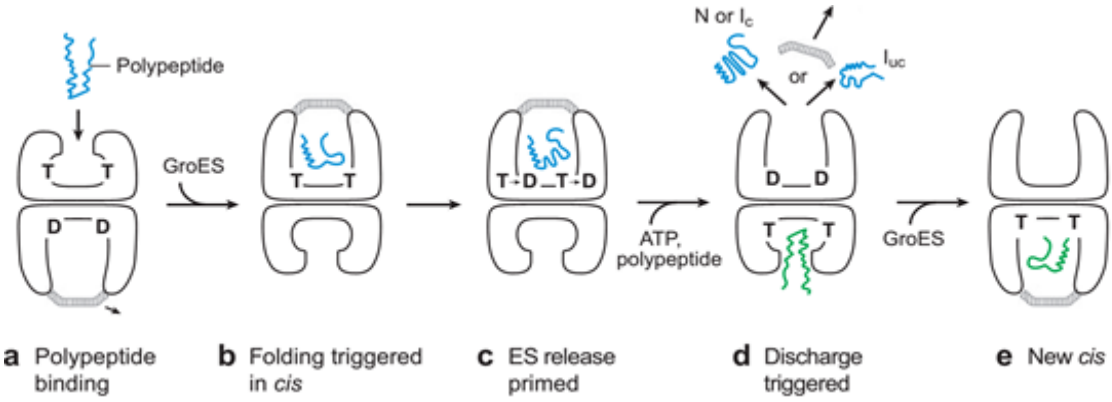

Figure 1.3 : Conformational cycle of the ATP-regulated GroEL-GroES: Asymmetric regulation takes place between the two rings in ATPase cycle (T denotes ATP-bound, D denotes ADP-bound rings). The ATP-bound ring accepts polypeptide substrate; subsequently the open face harbours the GroES. After encapsulation, the rigid body movements process releases polypeptide which may be in native (N), commited-intermediate (I_c) or uncommitted (I_{uc}) state. Concomitantly, the other ring binds ATP and polypeptide and new *cis* complex formed (Horwich et al., 2007).

Protein quality control system serves not only in protein folding, macromolecular assembly but also disaggregation of intertwined non-native protein clusters and reliance of targeting potentially detrimental proteins to proteolytic pathway (Mogk et al., 2015). Upon harsh circumstances such as heat stress, aggregation susceptibilty is escalated critically due to increased non-specific intramolecular interaction. Hsp100/Clp is ATP-regulated hexameric chaperone family which serves as aggregation-solubilizer machine and component of protease complex, function based on principle of unfolding, belonging to AAA+ protein superfamily (Neuwald et al., 1999). Members of the superfamily share the same domain (AAA) which is about 230 amino acids in length, facilitating oligomerization and containing

conserved Walker A and Walker B motifs to bind and hydrolyse ATP. The members of Hsp100 family are divided on basis of the number of AAA domain per promoter, which may be one or two, and unique extra domain that gifts the member functional specifity in interaction with substrates (Mogk et al., 2015).

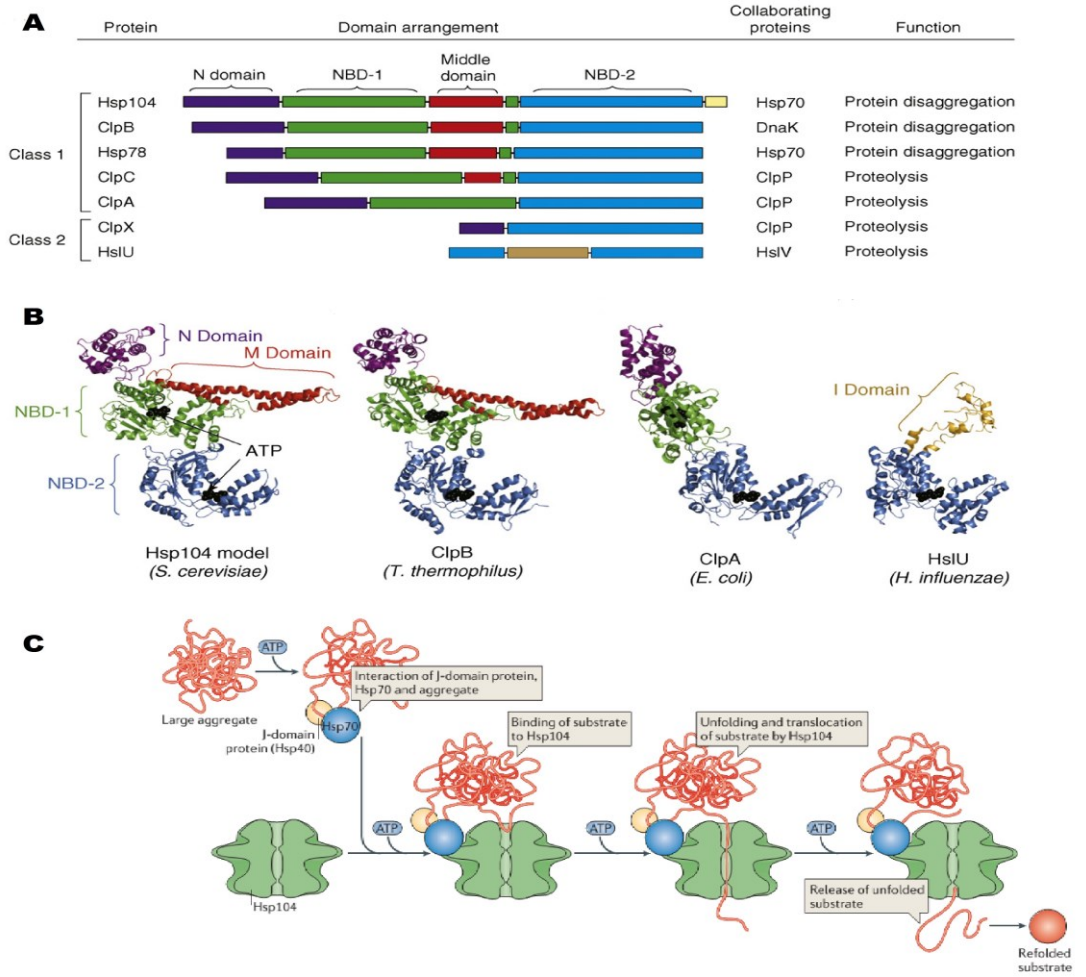

Figure 1.4 : Domain organisation and structure of Hsp100 family. a) Hsp100 family is classified in respect of variety in number of nucleotide binding domain (NBD). Class I includes one NBD whereas Class II has two NBDs. Each member may contain unique domain which plays role in substrate interaction and associated with specialized function (Doyle & Wickner, 2009). b) Crystal structures of *T.thermophilus* ClpB (PDB ID: 1QVR), *E.coli* ClpA (PDB ID: 1KSF) and *H.influenza* HslU (PDB ID: 1E94). *S.cerevisiae* Hsp104 structure is based on Swiss-model, generated from *T.thermophilus* ClpB (PDB ID: 1QVR) (Doyle & Wickner, 2009). c) Functional representation of bi-chaperone complex (Doyle et al., 2013).

Hsp104, also referred to as ClpB in *E. coli* is a member of Hsp100 chaperone family, specialized to reverse aggregation to counteract against stress conditions. The structure of Hsp104 is composed of N-terminal domain followed by nucleotide-binding domain (NBD-1), a middle domain (M-domain) and another nucleotide-binding domain (NBD-2), respectively (Lee et al., 2003). Both NBDs bind and

hydrolyse ATP. Oligomeric state is stabilized by ATP binding. However, the Hsp104 mode of action in remodelling aggregates has not been fully understood (Doyle & Wickner, 2009). Regarding the function of ATP, it has been stated that ATP binding provides Hsp104 to adopt 'holdase' activity and subsequent hydrolysis changes the function to 'unfoldase' (Doyle et al., 2007). Same study has indicated that binding of slowly hydrolysed ATP analogue, ATP-γS provides remodelling for some substrates but does not account for some others which require the hydrolysis. Consequently, it has been suggested that the versatility in mechanism provided by each step, ATP binding and hydrolysis expands the repertoire of aggregated substrates which can be dealt with upon stress conditions (Doyle et al., 2007). Additionally, Hsp104 is not mere disaggregation machine, works in concert with Hsp70 and Hsp40 (JPDs). The complex is referred to as 'bi-chaperone system' by which the Hsp70 acts prior to Hsp104, controlling the recruitment of Hsp104 at the vicinity of aggregate clusters (Mogk et al., 2015). Hsp104-Hsp70 binding interface has been reported by a NMR spectroscopy, overlapping the binding interface of NEFs-Hsp70 which indicates that NEFs are not required in disaggregation process facilitated by Hsp70-Hsp104 complex (Rosenzweig et al., 2013). Remarkably, the activation of Hsp104 requires more than one Hsp70 binding to Hsp104 (Mogk et al., 2015).

ClpP is the first discovered member of Hsp100 as a component of the protease system (Fujimura et al., 1987). It is proteolytic central component of ATP-dependent protease system, and capped by a set of Clp members such as ClpA and ClpX to form ClpAP and ClpXP complexes, respectively (Doyle & Wickner, 2009). ClpP has been reported to bind both ClpA and ClpX simultaneously via its opposite sides to form active hybrid compex, ClpXAP (Ortega et al., 2004). This bi-functional protease system whose both ends harbouring different modulator is able to target different set of polypeptides independently (Ortega et al., 2004).

There are diverse classes of chaperone families, of which each serves with unique mechanism, of some use catalytic power of the ATPase activity to drive different conformational states to deal with their authentic clients, and of some show oligomeric character. Addition to the families detailed above, the cell hosts many small heat shock (sHsp) families such as Hsp26 in *S. cerevisiae* and α-crystallin in mammalians, preventing and refolding the aggregation in concert with other ATP-dependent chaperones (Bakthisaran et al., 2015).

1.3. The Chaperone Hsp90

Hsp90 is a conserved and abundant molecular chaperone that regulates the final maturation and activity of various clients which mainly function in cellular stress response, proliferation and hormone signalling (Young et al., 2001; Wandinger et al., 2008). Some of these clients are implicated in cancer progression, which makes Hsp90 a potential target for therapeutic approaches (Solit & Rosen, 2006). Hsp90 is an essential protein in eukaryotes whereas the prokaryotic homologue of Hsp90, HtpG, is dispensable. In some cellular compartments Hsp90 paralogues are present: In the ER, the paralogue is called Grp94 and in mitochondria Trap1.

Hsp90 interacts with more than 200 clients (Li et al. 2012). In contrast to other chaperones, Hsp90 binds its clients without having a preference for specific structures. The molecular basis of client recognition of Hsp90 is largely unknown (Karagöz & Rudiger, 2015). Next to largely folded clients, Hsp90 has been reported to interact with partially folded and intrinsically disordered clients such as p53 and Tau, respectively (Karagöz & Rudiger, 2015).

More than 20 co-chaperones exert a regulatory influence on Hsp90 by facilitating client-loading conformation, the recruitment of clients and modulation of the ATPase cycle. The cooperation with various co-chaperones enables Hsp90 to be a rather versatile chaperone dealing with structurally diverse clients (Röhl et al., 2013). Even though many aspects of co-chaperone effect on Hsp90 as in asymmetric complex have not been clarified yet, the ordered progression in co-chaperone interaction has been implicated in maturation of certain clients (Röhl et al., 2013).

1.3.1 Structure and conformational change of the Hsp90

Hsp90 exerts its cellular functions as obligate homodimer of which each protomer consists of three domains. The N-terminal domain has a molecular weight of approximately 25 kDa and contains a binding pocket for ATP. Various drugs have been developed that bind in this pocket (Solit & Rosen, 2006). A charged linker at the boundary between N-terminal and middle domain is implicated in regulation of Hsp90 (Tsutsumi et al., 2012). The middle domain (referred to as M domain) is known as to interact with various clients and co-chaperones (Karagoz & Rudiger, 2015). The most important function of the C-terminal domain is to mediate the dimerization of the two protomers (Li et al., 2012). Hsp90 is a member of the GHKL

ATPase family, members of which share a similar ATP binding pocket (Dutta et al., 2000). Even though the domain organisation is highly conserved among the Hsp90 homologues (Figure 2), each homologue has differences in sequence and structure. These differences are tightly associated with the unique functional properties of each homologue (Johnson, 2012).

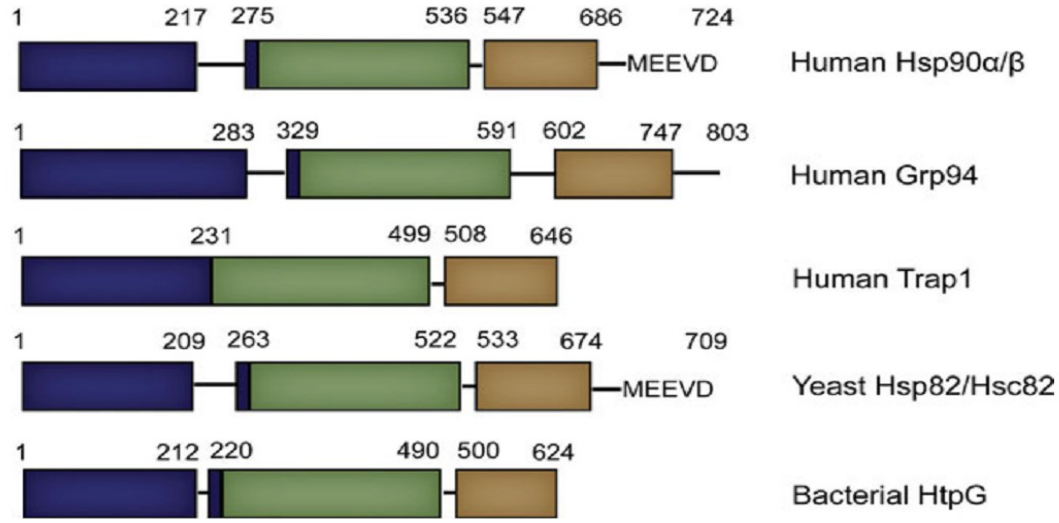

Figure 1.5 : Domain organisation of the Hsp90 homologues. The N-domain is coloured in blue, the M-domain in green and the C-domain in brown (Krukenberg et al., 2011).

Hsp90 shows an ATP-dependent chaperone function and its ATPase activity plays a crucial role for viability in yeast. It is reported that the ATPase activity is essential for maturation of hormone receptors and kinases (Panaretou et al., 1998). Both structural and biophysical studies revealed that Hsp90 adopts a set of structurally distinct conformations driven by nucleotide identity and ATP hydrolysis (Ali et al., 2006; Shiau et al., 2006; Hessling et al., 2009; Mickler et al., 2009). In the absence of nucleotide, Hsp90 adopts an open V-shaped conformation which exhibits a large solvent exposed surface. Binding of ATP to the pocket in the N-domain makes the lid closure favourable and causes the formation of the first intermediate state. Subsequent structural arrangements lead to the closed conformation, in which the N-domains of each protomer dimerizes and contacts between N and M domain are facilitated, resulting in hydrolysis of bound ATP. It should be noted that Hsp90 family is higly dynamic and able to adopt all cycle conformations in the absence of nucleotide. In other words, nucleotide does not dictate a certain conformation (Southworth et al., 2008; Krukenberg et al., 2009; Mickler et al., 2009).

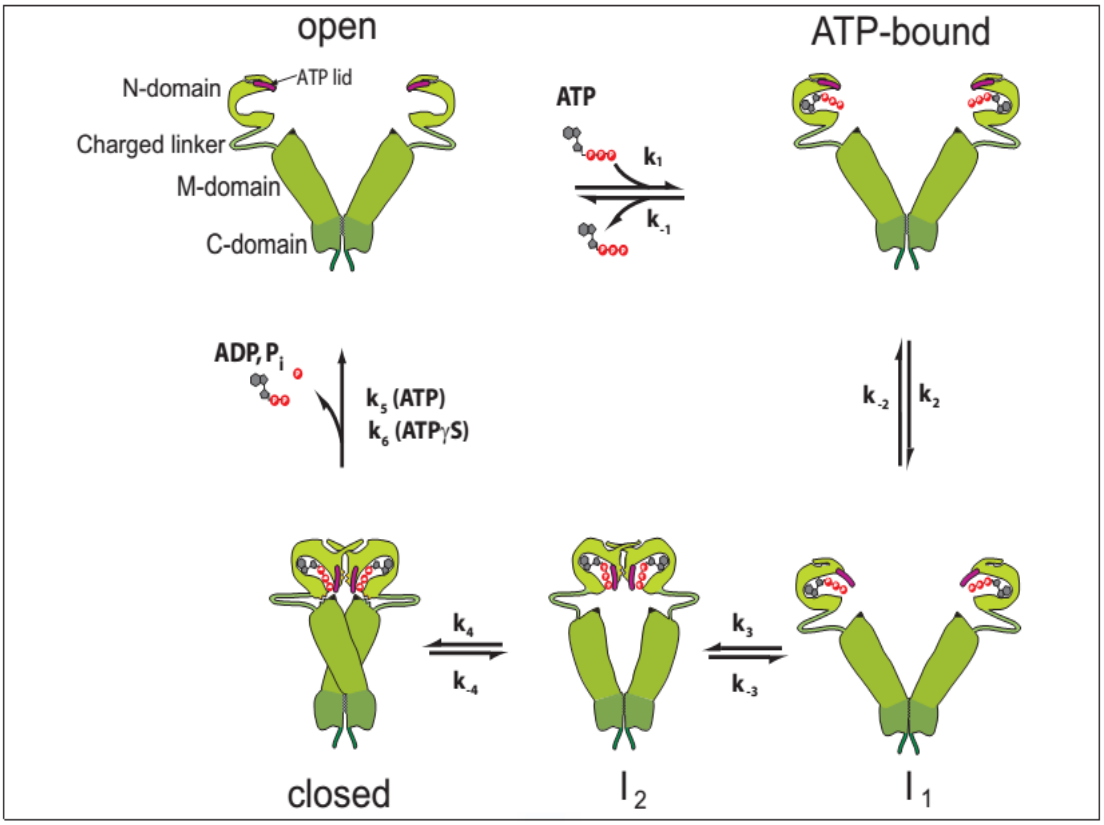

Figure 1.6 : The ATPase cycle of Hsp90: The cycle begins with the binding of ATP into the nucleotide binding pocket of the N-domain with diffusion-collision effect. The lid closes over the ATP and Hsp90 adopts the first intermediate state (I_1). The second intermediate state (I_2) is formed by N-domain dimerization. Subsequent rearrangements drive Hsp90 into a more compact closed state, in which N- and M- domains contact, which makes ATP hydrolysis favourable. After release of ADP and P_i, the cycle ends and Hsp90 adopts the open state and the cycle begins again (Li & Buchner, 2013).

The ATPase activity of Hsp90 is slower than those of many other ATP-dependent chaperone proteins. Yeast Hsp90 hydrolyses about one ATP molecule per minute, whereas the human homologue is approximately ten times slower (Panaretou et al., 1998; Richter et al., 2008). Concerning the human Hsp90, the possible reasons behind the weak ATPase rate have been proposed to be caused from either its distinct conformational equlibrium or rate of hydrolysis and ADP dissociation. Additionally, the kinetic data which have been presented up to now showed that the rate limiting step of human Hsp90 is the chemical breakage of ATP rather than dissociation of ADP. Regarding the relevance among the cycle elements, while the ATPase activity of the Hsp90 is essential for its function in client maturation, along with various co-chaperones the client binding regulates ATPase cycle of Hsp90 (McLaughlin et al., 2004). The extent to which concert of the client, co-chaperone and Hsp90 triad is associated with ATPase cycle is under investigation of current studies.

1.3.2 The endoplasmic reticulum paralogue of Hsp90, Grp94

Grp94, also known as gp96 or endoplasmin, is an essential chaperone protein which is expressed ubiquitously in the ER. It is required for the maturation of various secretory and membrane proteins. The clients of Grp94 are implicated in signal transduction and immune response (Pratt & Toft, 2003; Pearl & Prodromou, 2006). A set of clients associated with the immune system has been reported, including IgGs, integrins and Toll-like receptors (Melnick et al., 1994; Randow & Seed, 2001; Yang et al., 2007). Most importantly, Grp94 plays a role in the development of metazoans and it is not present in unicellular organisms (Eletto et al., 2010). However, Grp94 knock-down in mammalian cell culture leads to slow growth without deficiency in surface receptor expression and differentiation (Ostrovsky et al., 2009; Wanderling et al., 2007; Randow & Seed, 2001).

Unlike its cytoplasmic counterparts, Grp94 is able to bind calcium (Biswas et al., 2007). Grp94 seems to bind between 16 and 28 Ca^{2+} molecules (Macer et al., 1988; Van et al., 1989) and over-expression of it is reported to compensate the toxic effect of a high intracellular Ca^{2+} concentration (Vitadello et al., 2003).

Since the ER differs from the cytosol, Grp94 must have evolved to deal with a different client spectrum. The first identified clients of Grp94 were intermediates of the immunoglobin family, which also interacts with the ER chaperone BiP in a sequential manner (Melnick et al., 1994). Furthermore, it has been reported that the maturation of insulin-like proteins, IGF-1 and IGF-2 are dependent on Grp94 (Ostrovsky et al., 2009). Although it has long been an enigma whether Grp94 has a *bona fide* ATPase activity, a set of studies has proposed a role of ATP hydrolysis in client maturation. Mutation of either the putative catalytic residue E103 or the ATP-binding residue D149 abolishes Toll-like receptor expression while these mutations have no effect on integrin expression (Randow & Seed, 2001). However, later, an accessory protein was reported to be a potential co-chaperone of Grp94 and implicated in proper expression of Toll-like receptors. Since the putative catalytic residue E103 is indispensable for interaction with this suspected co-chaperone, the co-chaperone interaction rather than the ATPase activity might be decisive in the maturation of Toll-like receptors.

It has been clarified by two independent studies that Grp94 has an intrinsic ATPase activity (Frey et al., 2007; Dollins et al., 2007). In one study the kinetic parameters of Grp94 were elucidated, and it was reported that the ATPase rate of Grp94 is comparable to that of the yeast counterpart, K_{cat}=0.36 min^{-1}. The same study also showed that Grp94 binds tighter to nucleotides than the other Hsp90 family members (Frey et al., 2007). Another study has given structural insights of nucleotide-bound Grp94 (Dollins et al., 2007). The study also includes a measurement of the ATPase rate of Grp94 and chimeric constructs in which the three domains are swapped between Grp94 and cytosolic yeast Hsp90. In this study, the ATPase rate is assessed as yielding K_{cat}=0.02 min^{-1}, unlike the rate determined in Frey's article. Besides, the ATPase rates of the chimeric constructs suggest that the difference in the ATPase rate between Grp94 and yeast Hs90 mainly arise from the N-domain (Dollins et al., 2007).

Dollins' paper has great importance since has disclosed the first crystal data of ADP- and AMP-PNP-bound full-length Grp94 at 2.4 Å resolution. Interestingly, this study shows that there is no significant difference between AMP-PNP- and ADP-bound Grp94, which both adopted to the twisted V conformation reminiscent of an intermediate between apo HtpG and AMP-PNP-bound yeast Hsp90 crystal structures. Intriguingly, in the crystal data, the putative catalytic residue from M-domain, R488 is positioned more than 21 Å away from the γ-phosphate of the bound AMP-PNP, which seems to have distant proximity for interaction. For proper alignment of the putative catalytic residues, it appears that the M-domain would need to swing 90^{o} towards the nucleotide. The study thus points out that either clients or a co-chaperone may play central role in triggering ATP hydrolysis (Dollins et al., 2007).

The effect of nucleotide binding on the conformation of Grp94 has been investigated extensively with various techniques including SAXS, EM, co-crystallization and biochemical experiments (Dollins et al., 2007; Frey et al., 2007; Immormino et al., 2004; Krukenberg et al., 2009; Soldano et al., 2003). A SAXS study has shown that in solution, the spectrum of Grp94 conformations resembles that of Hsc82 and Hsp90 α (Krukenberg et al., 2009). Notably, the same study reported that addition of nucleotide cause a slight shift to the closed conformation of Grp94, which does not reach the extent of inducable form of cytosolic yeast counterpart, Hsp82

(Krukenberg et al., 2009). Unsuprisingly, among the different members of Hsp90 family, the level of the shifts to the closed conformation are correlated with the ATP hydrolysis powers.

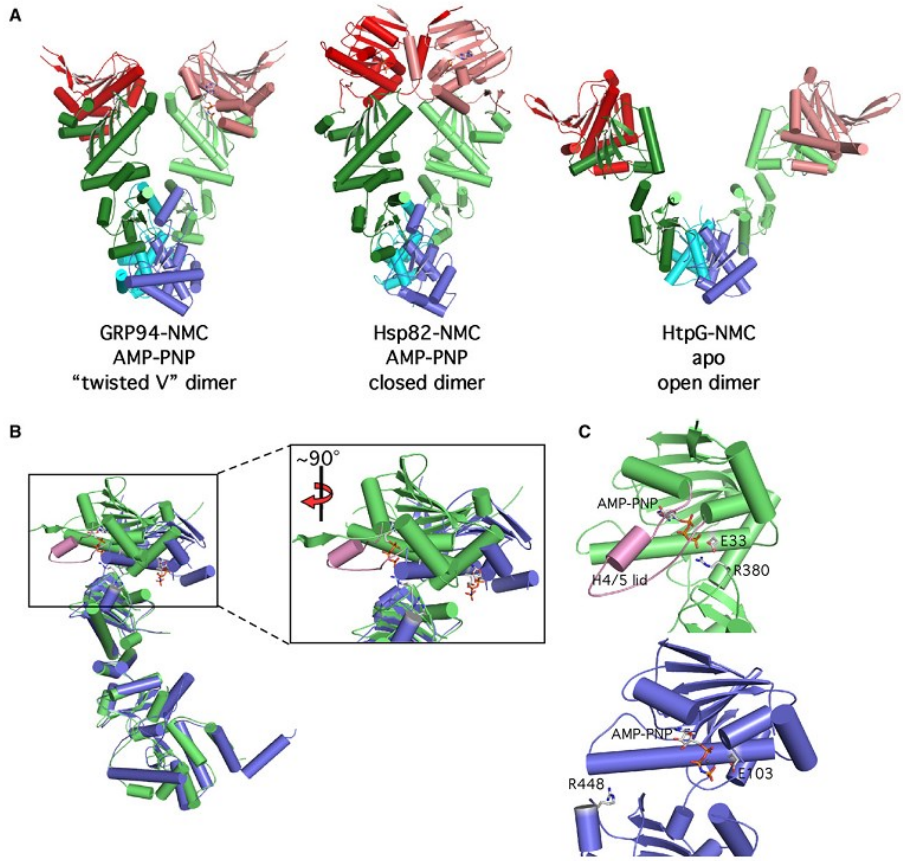

Figure 1.7 : Structural comparison of mamalian Grp94, yeast Hsp90 and bacterial HtpG. a) Crystal structure of AMP-PNP bound canine Grp94, the closed state of yeast Hsp90 and the apo form of HtpG. B) N-domain structural alignment of AMP-PNP- bound Grp94 (blue) and AMP-PNP-bound conformation of yeast Hsp90 (green). C) The positioning of putative catalytic residues of AMP-PNP bound Grp94 (blue) and yeast Hsp90 (green). R448 residue of Grp94 seems to have relatively much distance than do its cytosolic counterpart (Dollins et al., 2007).

Aid to the structural explanation of the ATPase activity of the mamalian Grp94 and discovering an unseen twisted conformation, the structure also revealed a potential client-binding site positioned in an alpha-helix, composed of central Methionine (M-M, residues 658 and 662) pair and four solvent-expose aromatic residues (Y652, Y654, Y677 and Y678). The role of binding of the client or any unexplored co-chaperone has been proposed to be triggering factor that enables Grp94 exceeds transition energy barrier for N- terminal dimerization. Although for cytosolic yeast Hsp90, it has been earlier elucidated that the same conserved binding platform takes

a part in interaction with glucocorticoid, its role in Grp94 is still unknown (Dollins et al., 2007).

1.4 pERp1/MZB1

Perp1, also called as MZB1 is novel lymphocyte-specific 18 kDa ER protein which is implicated in immunoglobin folding, assembly and secretion. (Shimizu et al.,2009; Anken et al., 2009). Knock-down and upregulation assays revealed that pERp1 is a essential folding factor for IgM, which may act as unique oxidoreductase or co-chaperone of BiP complex (Anken et al., 2009; Rosenbaum et al., 2014).

During differentiation of the B cell to plasma cell, a set of striking morphological changes occur and the B cell is adapted to produce large amount of antibody (Anken et al., 2009). To demand daily antibody secretion as high as its own mass, ER is expanded accompanied by upregulation of protein quality control and proteolysis components. Producing antibodies in the ER needs to be processed by oxidative folding and accurately assembled to gain native structure and function. Protein disulfide isomerase (PDI), ERp57 and oxidoreductases are upregulated to support formation, reduction and isomerization of intra- and inter-chain disulfide bonds, effectively (Wiest et al., 1990; Anken et al., 2003; Shaffer et al., 2004). Concert among these components with significant increase in their quantity plays crucial role in differentiation of B cell becoming antibody secretion machinery. pERp1 is newly discovered protein which is upregulated over the course of B cell differentiation, reaching the extent as much as BiP in amount (Anken et al., 2009). The precise mode of pERp1's action is still elusive.

pERp1 is highly expressed in spleen relative to other tissues. It includes 6 cysteines in total and CXXC motif which is hallmark of oxidoreductases. *In vitro* thiol-reductase activity assay revealed that pERp1 has modest oxidoreductase activity. In addition, pulse-chase and mass spectrometry analyses discovered that CXXC interacts another motif $C(X)_6C$, forms long-range intrachain disulfide bond which seemingly stabilizes overall structure (Anken et al., 2009). PERp1 interacts with both heavy and light chain of the IgM both covalently and noncovalently (Shimizu et al., 2009). Since pERp1 is able to bind IgM monomers noncovalently, it is proposed that pERp1 may function as molecular chaperone. According to other scenario, pERp1 may display greater oxidoreductase activity in the condition of ER compared to *in*

vitro and may be a cell-line specific oxidoreductase which differs from other known ones (Anken et al., 2009).

Figure 1.8 : Sequence and structure of the pERp1. a) Amino acid sequence of *Mus musculus* pERp1. Italic sequence is target sequence. 6 conserved cysteines are with asterisks, and CXXC motif is in bold. Underlined sequences convey mass spectrometry obtained polypeptides. Double underlined 'REEL' is retention sequence (Shimizu et al., 2009). b) Representation of disulfide bonded structure of pERp1 (Anken et al., 2009).

It has been long known that Grp94 serves as chaperone of IgM light chain by which the interaction followed by that of Hsp70 member, BİP (Binding Immunoglobin Protein) in a sequential manner (Melnick et al., 1994). The same study has disclosed that the immunoglobin light chain binding to Grp94 has distinct characteristics compared to BİP, respecting life-time of interaction and oxidation state of the clients. Remarkably, Grp94 binds the oxidized immunoglobin intermediates with relatively longer-standing time course with regard to BİP which binds early intermediates promiscously. The authors highlight within a remark which claims that Grp94 assists the maturation of immunoglobins with more advanced action and mostly function as an assembler of the chains (Melnick et al., 1994). Another study which is more latterly published, showed that Grp94 is strictly dependent on pERp1 for the maturation of the mHC in ER stress condition stimulated by tunicamycin. The study mainly revealed that the interplay between pERp1 and Grp94 is essential for the fidelity of immunoglobin assembly and secretion. This data brings along with a rising question as to whether it is co-chaperone of ER Hsp90, Grp94 (Rosenbaum et al., 2014). However, there is not enough study which has examined it in aspects of molecular structure and biophysics.

1.5 Aim of the Study

In the context of study, it is aimed to shed light on long standing elusive point of Grp94 as to whether Grp94 is regulated by a co-chaperone influencing the ATPase cycle. In a set of previous studies, Grp94 has been shown to interact with immunoglobin intermediates (Melnick et al., 1994). Similarly, pERp1 seems to play a central role in immunoglobin maturation, assembly and secretation (Shimizu et al.,2009; Anken et al., 2009). Hereby, the question regarding if these two components of ER are in concert to deal with immunoglobin folding rises to be answered with molecular mechanistic details.

In this thesis, an initial step has been taken by steady state kinetics of *Canis lupus* Grp94 conducted with *Mus musculus* pERp1 in order to discover further implications of interaction and regulatory effect of pERp1 on Grp94. Besides, a truncated ubiquitin-tagged Grp94 is constructed in order to be used in single molecule studies since wt Grp94 is not compatible to be stained by Atto 488 dye. Possible concequences resulted from tagging of Grp94 with truncated ubiquitin were investigated by regenerative ATPase assay with determining K_{cat} and K_m and circular dichorism techniques.

In order to show binding of pERp1 and Grp94, analytical size exclusion chromatography is operated with Superdex 200 10/300 GL column connected to HPLC system. This technique may let us check the possible oligomeric state of pERp1, even might open the way of using it in line with light scattering (SEC-MALS) to determine steochiometry of binding. Furthermore, it is aimed to perform aggregation assay by which a model temperature-reacted protein, citrate synthase has been used and whose aggregation state monitored by increase in absorbance at 360 nm. Possible effect of pERp1 itself and in combination with tagged Grp94 on aggregation let us make new inferences would be very indicative for investigation of further details.

All in all, steady state kinetics of wt Grp94, Ubi-Grp94-Ubi and combination of each with potential co-chaperone pERp1/MZB1 gave us first insight on Grp94 mode of action. Possible effect of pERp1 on kinetics of Grp94 might be sign of specific client loading conformation of Grp94 which is attained with the interaction. Furthermore, binding kinetic of pERp1 and Grp94 has been calculated by titration of pERp1 via

steady state ATPase activity measurements. The study is crucial to clarify the existence of a co-chaperone of Grp94 which has not been discovered yet. Since there is not a structural insight of the interaction presented in this thesis, the results can be considered as initial step of a project concerning indeterminate chaperone cycle of Grp94 and implication of pERp1-regulated maturation of immunoglobins by Grp94.

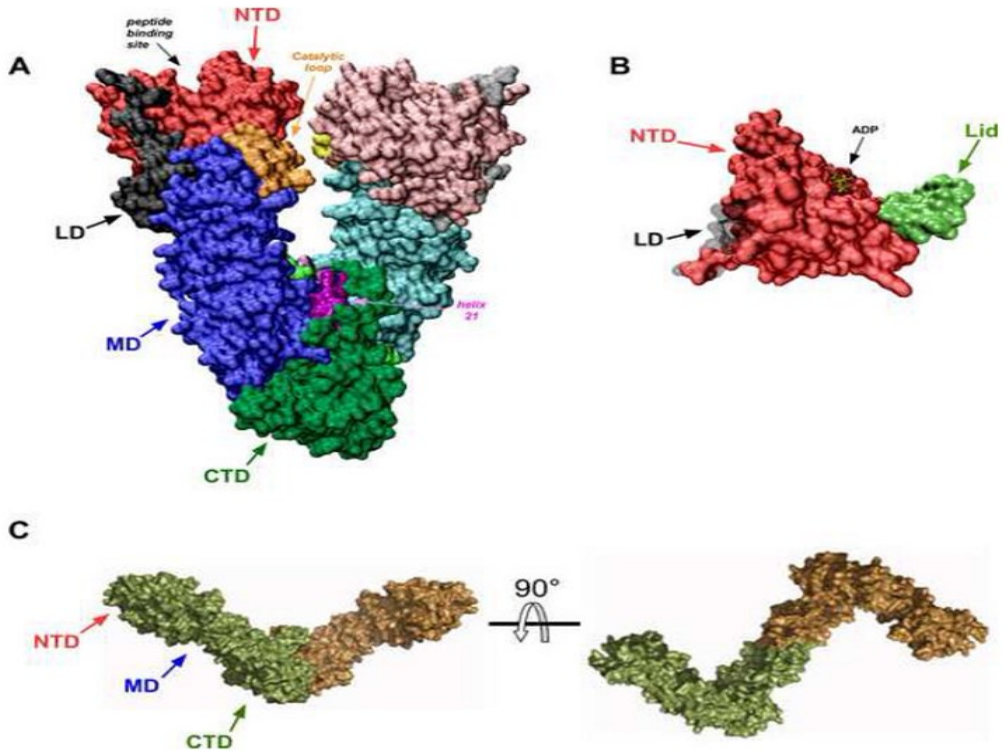

Figure 1.9 : Structure of Grp94. a) Twisted V conformation which is favourable in the presence of nucleotide (PDB ID: 2O1V). b) Nucleotide-bound N terminal domain of Grp94 (Eletto D., 2010). c) Extended chair-like conformation in solution (Krukenberg , 2009).

2. MATERIALS AND METHODS

2.1 Materials

2.1.1 Laboratory equipments

Laboratory equipments are shown in the Appendix A.

2.1.2 Chemicals and enzymes

Chemicals and enzymes used in the experiments are given in the Appendix B.

2.1.3 Buffers and solutions

Buffer and solution used in the experiments are given in the Appendix C.

2.1.4 Commercial kits

Commercial kits and used in the experiments are given in the Table 2.1.

Table 2.1: Commercial kits used in the experiments.

Kit	Sequence
Wizard^{R} PCR Clean-up Kit	Promega
Wizard^{R} Miniprep Kit	Promega
T4 Polymerase	New England BioLabs
1 kb DNA Ladder	Peqlab
Low-range SDS Marker	Biorad
High-range SDS Marker	Peqlab

2.1.5 Bacterial strains

E. coli Mach1 strain was used for plasmid amplification and BL21 DE3-CodonPlus™-RIL was transformed by respective plasmids in expression of both Grp94 constructs and pERp1. XL-1 Blue was transformed by one step sequence and ligation-independent cloning (SLIC) mixture at the last step.

2.2 Methods

2.2.1 Subcloning of Grp94

pET-21a plasmid including wt Grp94 was used in transformation of *E.coli* XL-1 Blue competent cells. 1 µL (approximately 90 ng) plasmid DNA was added to 50 µL competent cells taken from -80 ^{o}C. Then, plasmid - competent cell mixture was taken on ice for 30 minutes. Heat shock was applied at 42 ^{o}C for 45 seconds and the mixture was incubated on ice for 2 minutes. After these steps, 1 ml LB was added to mixture and incubated at 37 ^{o}C for 1 hour in shaker. Finally, the mixture was spread on ampicilin including LB plate (100 mg/L). The plate was incubated at 37 ^{o}C for 16 hours. As final step, a single colony on plate was inoculated into 5 ml LB and after overnight incubation at 37 ^{o}C plasmid purification was performed by protocol of Promega Miniprep Kit^{R}.

wt Grp94 gene of interest was amplified from pET-21a by PCR. Used primers were designed as being compatible with one step sequence and ligation-independent cloning (SLIC) protocol (Table 2.2).

Table 2.2: PCR primers compatible with SLIC.

Primers (Homology with Pet28a vector)	**Sequence**
Forward Primer (16 bp)	GAGAGGTGGT**GAGCTC**gacgatgaagtcgatgtg
Reverse Primer (18 bp)	GAAGATCTGCAT**AAGCTT**taattcatctttttcagctgtag

pET-28a including ubuquitin-tagged Hsp82 purified by using identical approach. Purified pET-28a plasmid double digested by SacI and HindIII in order to eleminate Hsp82 presesent in the plasmid, run on 1% agarose gel afterwards. Respective part of gel was cut and restricted pET-28a was taken out, subsequently cleaned up to perform SLIC cloning with Grp94 PCR product. SLIC mixture was introduced with XL-1 Blue strain and transformation was performed as explained previously.

SLIC method mainly depends on preparation of insert gene with 15 bp or more extension homologous to each flank of linearized vector. Linearization of vector can be performed by either restriction enzymes or inverse PCR. Linearized vector and insert gene are incubated 2.5 min accompanied by T4 polymerase which function as generator of elongation of 5' overhangs. It is a cloning method highly comparable to

other methods including ligation-dependent cloning methods in terms of efficiency, economy of time and usability (For the protocol see Table 2.3). It is highly compatible for high-throughput genomic studies (Jeong et al., 2012).

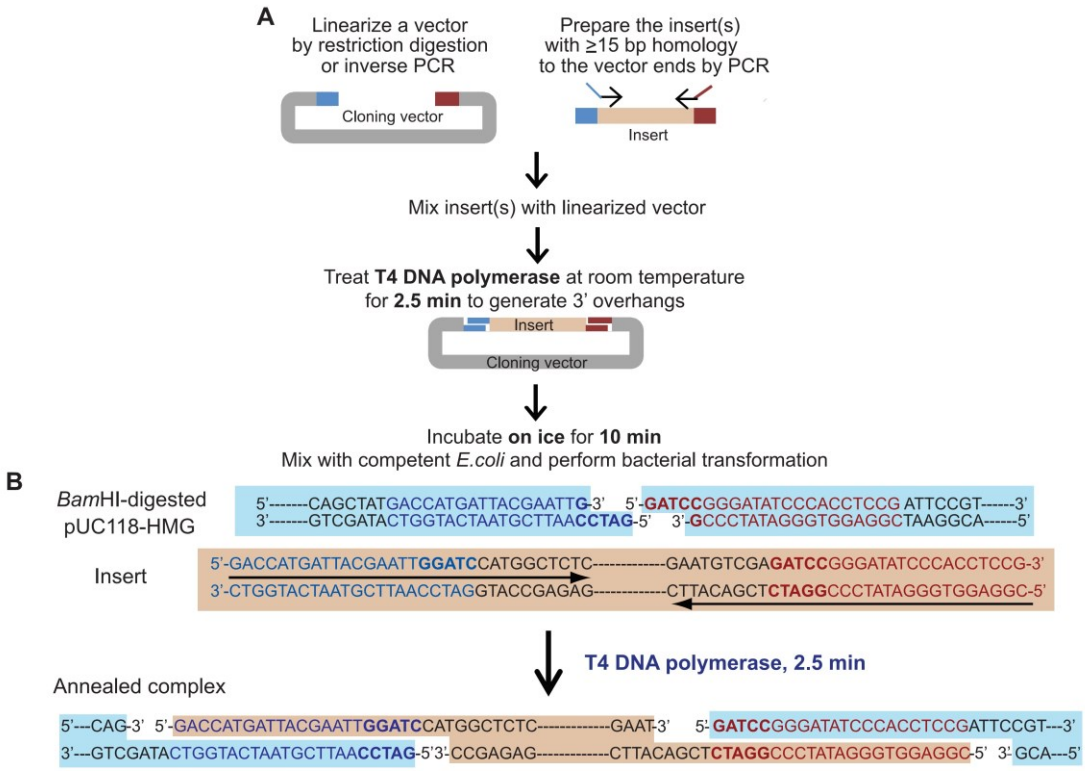

Figure 2.1 : Overview of one-step SLIC. a) Steps in SLIC method: Firstly, the vector aimed to be introduced by interested gene is linearized by enzymatic digestion or inverse PCR. Insert gene is prepared as to have at least 15 bp homology with the vector. Processed vector and insert are mixed and T4 polymerase is treated with additional components. After 10 minutes, bacterial transformation is carried out. b) Annealed parts of vector and insert gene with overhangs. Homologous segments have same colour (Jeong et al., 2012).

Table 2.3: PCR and SLIC protocols.

PCR	SLIC
1 µl Template (pET-21a)	50 ng Digested Vector (pET-28a)
1 µl Primer (Each)	1:8 Molar Excess of PCR Insert (Grp94)
5 µl 10x Pfu Buffer	1 µl NEB2 Buffer
39.5 µl H_20	1 µ 10x NEB BSA
1.5 µl dNTPs (10 µM each)	0.4 µl NEB T4 Polymerase
1 µl Pfu Polymerase	H_2O adjusted to 10 µl final volume

2.2.2 Plasmid transformation

The pET-28a including Ubi-Grp94-Ubi and pET-21a-Grp94 were transformed into *E. coli* BL21 DE3-CodonPlus™-RIL cell strain by similar transformation protocol as in that of XL-1 Blue transformation that was explained in 2.2.1. Unlike pET-21a, pET-28a has resistance against kanamycin.

2.2.3 Expression of wt Grp94, Ubi-Grp94-Ubi and pERp1

After the transformation, *E.coli* BL21 DE3-CodonPlus™-RIL cells, taken from one colony, were incubated at 37 ^{0}C for 16 hours in 50 mL LB medium containing ampicillin for wt Grp94 containing pET21-a or kanamycin for Ubi-Grp94-Ubi containing pET-28a. After 16 hours, 15 mL of growth was appended into 4L LB including respective antibiotics. Then, the culture was incubated at 37 ^{0}C until OD_{600}=0.8. Once OD reached 0.8, 1 mM IPTG was added to medium for induction. Before addition of IPTG, 1 mL sample was taken to eppendorf as a negative control. After 3-4 hours growth, cells were centrifuged at 6000 rpm for 30 minutes. Later, supernatant was discarded and cells were resuspended with resuspension buffer. Finally, resuspended cells were stored at -20 ^{0}C.

pET-32a including Trx-Tag_pERp1 sequence was used for transformation. Induction was carried with addition of 0.5 mM IPTG as final concentration when OD reached 0.5. The growth was incubated at 37 ^{0}C for 16 hours.

2.2.4 SDS-PAGE

To perform SDS-PAGE in order to check induction and purification level, 15 % and 10 % separation gels were used for pERp1 and Grp94 constructs, respectively. After electphoresis process, gels were stained by comassie blue solution, Fairbank A (15 minutes incubation after boiling) and destained by Fairbank D (5 minutes incubation after boiling).

Content of the SDS-gels is shown in Appendix C.

2.2.5 Disruption of the cells

French press as a physical method was carried out to disrupt cells. Before the process MixG protease inhibitor cocktail and after 0,2 mM PMSF was added as final concentration.

2.2.6 Purification of Grp94, Ubi-Grp94-Ubi and pERp1

Protein purification was operated by fast protein liquid chromatography (FPLC). Three different separation steps were performed to achieve purified proteins. For wt Grp94, as a first step Q Sepherose^{TM} column was used in which washing was operated by Buffer A and elution by Buffer B. Collected elution was dialysed against Solution A to be loaded onto Resource Q^{TM} column in which gradient approach was operated into the fractions. As a final step, gel filtration chromatography (Hi-load 200pg GE Healthcare column) was performed with Buffer C.

Concerning Ubi-Grp94-Ubi, as a first step Ni-NTA HisTrap^{FF} column was used since the construct contain His-tag in the truncated ubiquitin tag positioned at C-terminal. Washing phase was carried out by Phosphate Buffer A, elution was collected with Phosphate Buffer B. Respective elution fractions were pooled and dialyzed against Buffer A, subsequently loaded onto Resource Q^{TM} column. With same protocol followed in purification of wt Grp94, the gel filtration chromatography (200pg GE Healthcare column) was applied to the elution.

pERp1 purification was started with IMAC by using HisTrap^{FF} with Phosphate Buffer A in washing and Phosphate Buffer B in elution as described for Ubi-Grp94-Ubi. Dialysis against Tris Buffer A is performed in order to polish the imidazole off. Subsequently, elution was loaded onto Resource Q^{TM} and FPLC was operated with Tris Buffer A and B. Gel filtration chromatography was performed by 75pg GE Healthcare column along with Tris Buffer A. Collected fractions were pooled, concentrated and subsequently dialyzed against Phosphate Buffer A. To separate TRX-Tag, TEV Protease was appended into pERp1 and incubated for overnight at 4 ^{0}C. One more HisTrap^{FF} was performed to get rid of His-tag including TRX-Tag. pERp1 is collected from flowthrough and dialysed against TRIS Storage buffer.

2.2.7 ATPase activity assay

ATPase activities of Grp94 constructs were measured by real-time monitoring of oxidation of NADH to NAD^{+}. Hydrolysis of ATP to ADP converts phosphoenolpyruvate (PEP) to pyruvate by catalyzation of pyruvate kinase (PK). Lactate dehydrogenase (LDL) converts pyruvate to lactate by converting NADH to NAD^{+}. Oxidation of NADH to NAD^{+} is proportional to ATP hydrolysis. ATPase activity can be observed by tracking decrease of NADH with extinction coefficiency

6200 $cm^{-1}M^{-1}$ at 340 nm by Cary UV Visible spectrophotometer. The reaction was carried out in 150 µL reaction mixture, containing ATPase buffer (40 mM HEPES/KOH, 150 mM KCl, 5 mM $MgCl_2$, 2 mM ATP, 1.02 mM PEP, 0.2 mM β-NADH, PK/LDH cocktail (9.94 U/mL PK-14.2 U/mL LDH), 3µM Grp94 protein. pH was adjusted to 7.5 and the each reaction took place at 30 ^{0}C. ATPase activity was calculated with following equation:

$$\text{ATPase rate } [min^{-1}] = - dA_{340}/dt \text{ [OD/min]} \times K^{-1}_{path} \times moles^{-1} \text{ ATPase}$$

As negative control, the competitive inhibitor of Grp94, 20 µM NECA was used and unspecific ATPase activity resulted from contamination was subtracted from the value of measurement without NECA. 3 independent measurements were performed for each experiment.

pERp1 and Grp94 constructs were incubated 15 mins together in ATPase buffer before the mixture was introduced to ATP. Additionally, to determine K_m value of Ubi-Grp94-Ubi same protocol has been used with measurements of ATPase activity in different concentration of ATP at 37 ^{0}C. K_{cat} values are fitted in respect of Michaelis Menten equation.

EC_{50} (Half maximal of effective concentration) is expected to be in good line with K_d value of pERp1 and Ubi-Grp94-Ubi has been evaluated titration of pERp1 into Ubi-Grp94-Ubi ATPase activity at 30 ^{0}C. 3 independent measurements are performed and mean values of K_{cat} were used and fitted to Michaelis Menten equation. It should be noted that first 10 minutes is taken into account to determine K_{cat} values in titration of pERp1.

2.2.8 Circular dichroism measurement

Circular Dichroism (CD) is a spectroscopy technique, based on scattering right and left handed polarized light which is absorbed by interested matter, outputting different intensity. Far UV CD studies gives clues about the secondary structure of proteins whereas near UV reveals fingerprint of tertiary structure since the number and solvent expose state of aromatic amino acids differ protein to protein. CD is versatile tool to investigate secondary structures of manipulated versions of a certain protein roughly to be compared with wild type.

In the context of this thesis, far UV CD studies were performed by Jasco-715 spectropolarimeter. Measurements were carried out at 20 ^{0}C in 0.2 cm cuvette. The

signals collected from 195 nm to 260 nm with 1 nm band width and 8 seconds integration time. Both constructs were dialyzed against 20 mM Hepes, 75 mM KCl, pH 7.5 before the measurements.

2.2.9 Citrate synthase aggregation assay

Citrate Synthase (CS) is a model protein which is aggregation prone in high temperature. What makes it convenient is that its aggregation progression can be simply monitored by both light scattering and absorbance at 360 nm. Molecular chaperones known as aggregation supressing component of cell. Even CS is not authentic client, Grp94 has versatile function in interacting with unstable proteins to keep them functional.

In this thesis, the effect of Grp94, pERp1 and their combination to aggregation of CS has been monitored by spectrophotometer at 360 nm. The temperature of system was adjusted to 43 ^{0}C which has been optimized and reported in literature (Buchner et al., 1991). 0.3 μM CS conducted to 1 μM Grp94 and 5 μM pERp1 both independently and in together. Reactions took place in Hepes Buffer (pH 7.5) with 150 μl volume and monitored by 50 minutes.

2.2.10 Analytical size exclusion chromatography

In order to show possible interaction of pERp1 and Grp94, analytical size exclusion (Superdex 200 10/300 GL) with HPLC system operated. Size exclusion chromatography works with the simple principle of that the proteins which have different molecular weight have different hydrodynamic volume. Each protein migrated with different rates in designed columns since high molecular weight protein or protein complexes relatively moves fast compared to the low molecular size proteins.

In our study, pERp1 and Grp94 has been independently subjected to Superdex 200 10/300 GL column in which buffer including 40 mM Hepes, 150 mM KCl, 5 mM $MgCl_2$ and 0.5 mM DTT (at pH 7.5) was loaded onto column before operating the proteins. Subsequently, the proteins were incubated together in 3 different conditions; at 8^{0}C and 37 ^{0}C for 45 minutes and with 10 mM $CaCl_2$ supply at 37 ^{0}C for 45 minutes. Incubated protein mix samples were applied to the same column with 0.5 ml/min flow rate. To determine molecular weight of possible interaction or

oligomeric states, Bio-Rad Gel Filtration Standard^{R} was subjected to the tool, independently.

3. RESULTS

The first aim of this thesis was to construct a plasmid in which Grp94 from *Canis lupus familiaris* is flanked by truncated *Gorilla gorilla* ubiquitin on the N- and C-terminal site. This led to a construct which will be referred to as Ubi-Grp94-Ubi. Ubi-Grp94-Ubi and wild-type (wt) Grp94 were then recombinantly expressed in *E.coli* and purified to assess the ATPase activity of both proteins. K_m value corresponding affinity of Ubi-Grp94-Ubi against ATP has been evaluated to be compared with previous work results (Frey et al., 2007). Additionally, ATP measurement was conducted with the potential Grp94 co-chaperone pERp1/MZB1 in order to reveal its possible influence on Grp94 ATPas kinetics. Steady state ATPase activities in respect of titration of pERp1 has been calculated and fit to the single exponential equation, aiming to determine EC_{50}. Apart from steady state kinetic measurement, pERp1, Ubi-Grp94-Ubi and combination of them were subjected to citrate synthase (CS) aggregation assay. Finally, the analytical size exclusion was operated to show interaction of pERp1 and Ubi-Grp94-Ubi and the oligomerization state of pERp1 in physiological conditions.

3.1 Grp94 is subcloned into pET-28a to construct Ubi-Grp94-Ubi

In order to produce the Ubi-Grp94-Ubi construct Grp94 PCR product was cloned into pET-28a vector with an Ubi-Hsp82-Ubi insert. The vector was double-digested with SacI and HindIII restriction enzymes. In used vector, both downstream of the HindIII restriction site and upstream of the SacI restriction site the same truncated ubiquitin tag is present. Hsp82 (which in the original construct had been cloned between the two ubiquitin tags) was cleaved out and gel purification was performed to get a digested pET-28a vector including the ubiquitin tags. The PCR of wt Grp94 was performed by using a pET-21a vector by primers compatible for sequence and ligation independent cloning (Jeong et al., 2012). Subsequently, the one step ligation-independent cloning (SLIC) protocol was carried out by using the cleaved pET-28a vector and the Grp94 PCR product. The reaction mixture was transformed into

competent XL-1 Blue strain. Insertion of wt Grp94 into pET-28a was confirmed by sequencing.

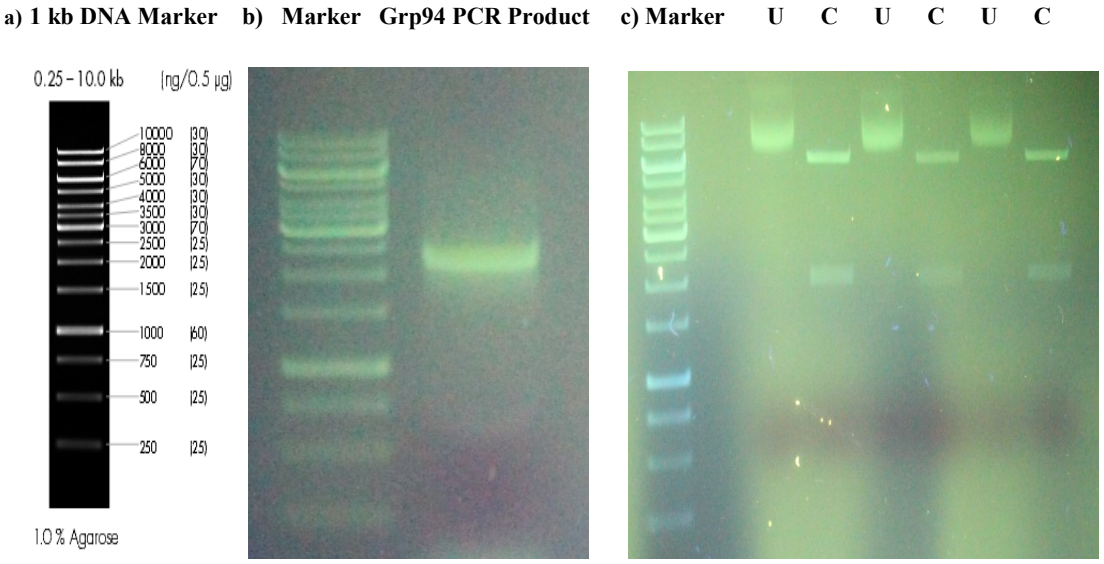

Figure 3.1 : Cloning of Ubi-Grp94-Ubi into the pET-28a vector. a) Peqlab 1 kb DNA Ladder^{R}. b) The Grp94 PCR product aimed to be cloned into a pET-28a vector. c) Hsp82 was cleaved out from the pET-28a vector including Ubi-Hsp82-Ubi sequence by double digestion with SacI and HindIII to produce a vector for Ubi-Grp94-Ubi cloning. C devotes cleaved and U devotes uncleaved pET-28a. After the cleavege, the ubiquitin tags still were present on the vector. The percentage of agarose gel is 1%.

3.2 Induction and Purification of Grp94 Constructs

Both the wt Grp94 and the Ubi-Grp94-Ubi constructs were expressed in BL21 DE3-CodonPlus™-RIL strain. 4 L of both strains in LB medium were grown until OD reaches 0.8 and protein expression was subsequently induced with 1 mM IPTG. After induction, the cells were incubated at 37 C^{o} for 3 hours. To purifiy wt Grp94, Q Sepharose^{R} column was used as a first anion-exchange step. Later, all elution fractions were used in second anion-exchange step, Resource^{TM} Q. As a final purification step, size exclusion (SEC) chromatography was applied to improve the purity. Since the C-terminal ubiquitin-tag in the Ubi-Grp94-Ubi construct includes a 6His-tag, a HisTrap^{TM} FF column was operated in the first step of Ubi-Grp94-Ubi protein purification. Thereafter, Resource^{TM} Q anion-exchange and SEC were performed, respectively. The purity levels of Grp94 and Ubi-Grp94 were different, Ni-NTA affinity chromatography seems to be an influential step in Ubi-Grp94-Ubi purification, and led to a better purify of Ubi-Grp94 compared to wt Grp94. 10% SDS-gels of the proteins are depicted in Figure 3.2 and Figure 3.3.

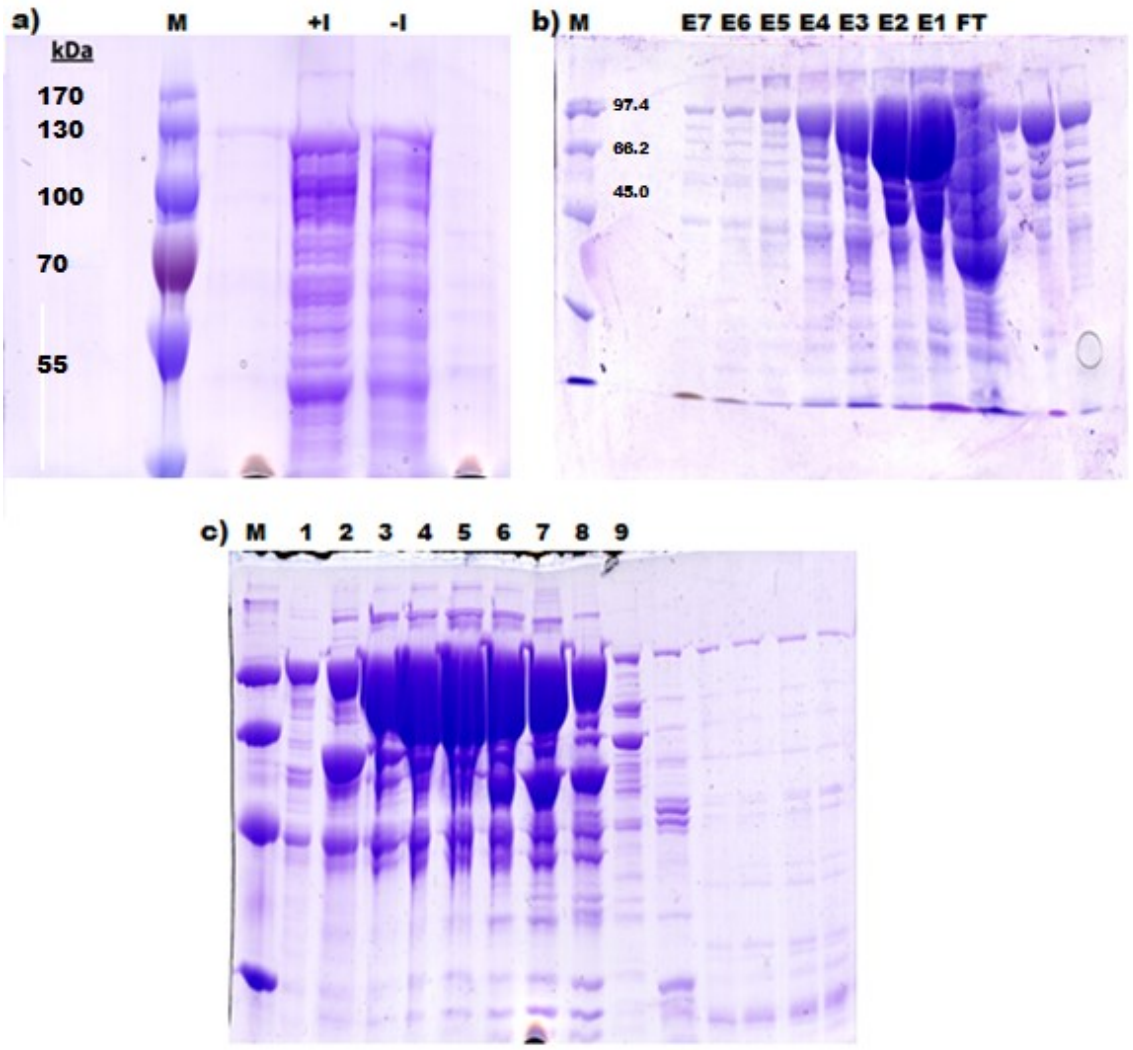

Figure 3.2 : SDS-PAGE analysis of the purification steps of wt Grp94. a) Protein expression analysis with total cell lysate: -I lane indicates the cell lysate before induction with 1 mM IPTG whereas +I shows the lysate after induction. b) Fractions of the Resource^{TM} Q anion-exchange purification step: The E1, E2, E3, E4, E5, E6 and E7 fractions were pooled and used in SEC. c) Fractions of size exclusion chromatography: The protein fractions in lanes 3, 4, 5 and 6 were pooled and used in further experiments.

On basis of the quantity of purified proteins and their similar induction profiles, it seems recovery of wt Grp94 is relatively higher than Ubi-Grp94-Ubi construct even there is a clear altitude of Ubi-Grp94-Ubi in purity (See figure 3.2 and 3.3 for SDS-PAGE analysis of respective protein's final purification extent). After sequential purification steps were fully completed for the constructs, the final amount has been evaluated approximately 17 mg for wt Grp94 whereas it was only about 6 mg for ubiquitin-tagged construct.

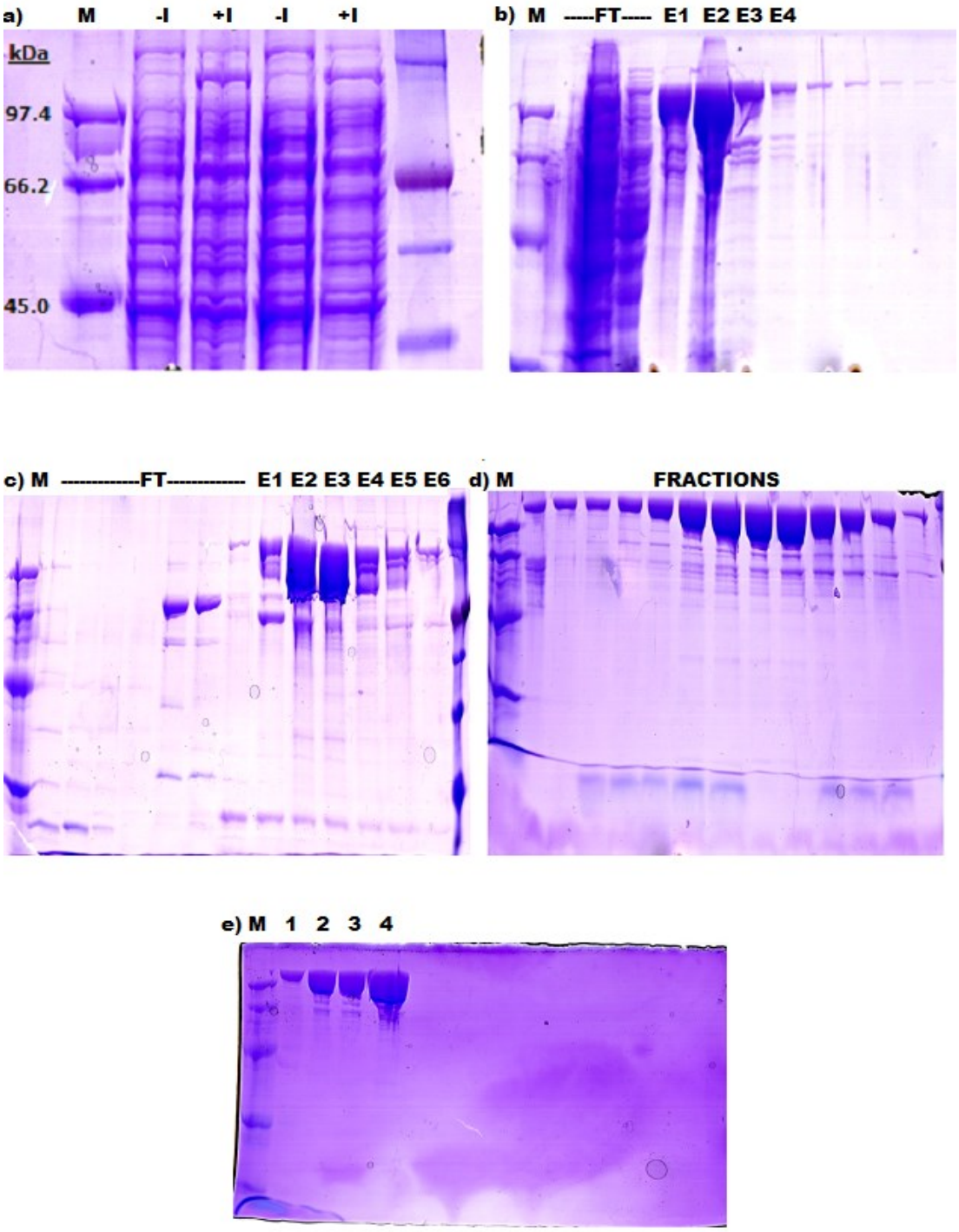

Figure 3.3 : SDS-PAGE analysis of the purification steps of Ubi-Grp94-Ubi. a) Protein expression analysis with total cell lysates: -I lane shows the lysate before induction. +I lanes depict the lysate after induction. b) Fractions of HisTrap^{FF} affinity chromatography: E1, E2 and E3 elution fractions were pooled to be used in next step (FT devotes 'flowthrough fractions'). c) Fractions of the Resource^{TM} Q anion-exchange purification step: E1, E2, E3, E4, E5 and E6 fractions were pooled to be used in SEC. d) Fractions of size exclusion chromatography: All fractions were pooled to be used in further experiments. e) Final purification samples in respect of increasing amount of load.

3.3 Induction and Purification of pERp1

pERp1 induction and purification successfully performed by using growth and purification protocols described in method sections 2.2.3 and 2.2.6. Respective gels below show gradual improvement in purification (Figure 3.4).

a) INDUCTION **b) HISTRAP^{FF} ELUTION**

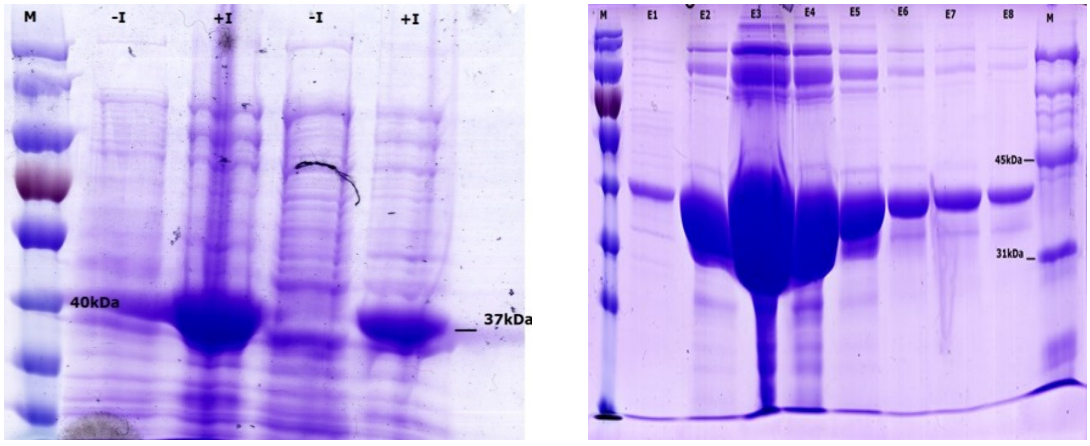

c) RESOURCE Q^{TM} ELUTION **d) SEC (75 pg)**

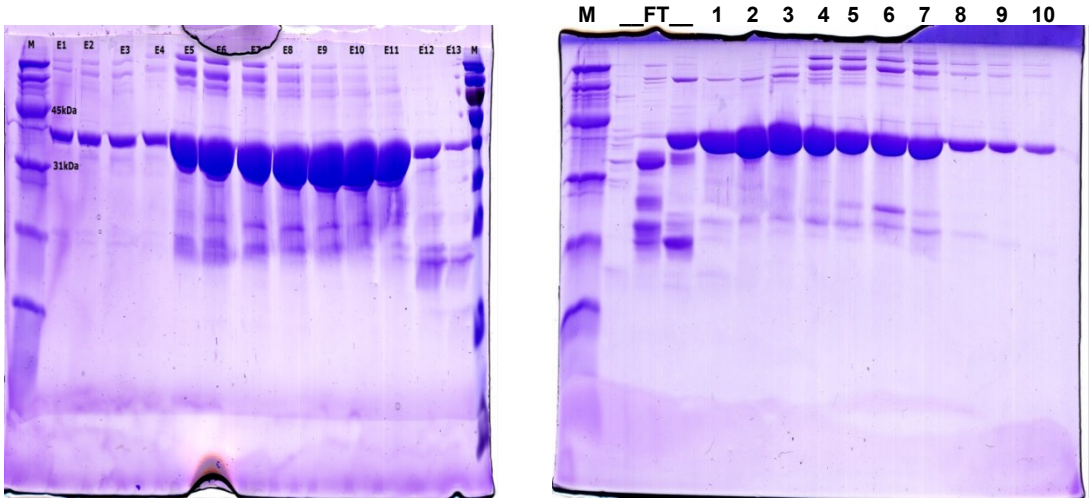

Figure 3.4 : SDS-PAGE analysis of the induction and purification steps of pERp1 before TEV cleavage. a) Protein expression analysis with total cell lysates: -I lanes are correspond to the lysate samples before induction. +I lanes are correspond to the lysate samples after induction. b) Fractions of HisTrap^{FF} affinity chromatography: E1 to E8 elution fractions were pooled to be used in next step. c) Fractions of the Resource^{TM} Q anion-exchange purification step: E1 to E13 fractions were pooled to be used in SEC. d) Fractions of size exclusion chromatography: The fractions in lanes 1 to 10 were pooled to be conducted to TEV enzymatic cleavage.

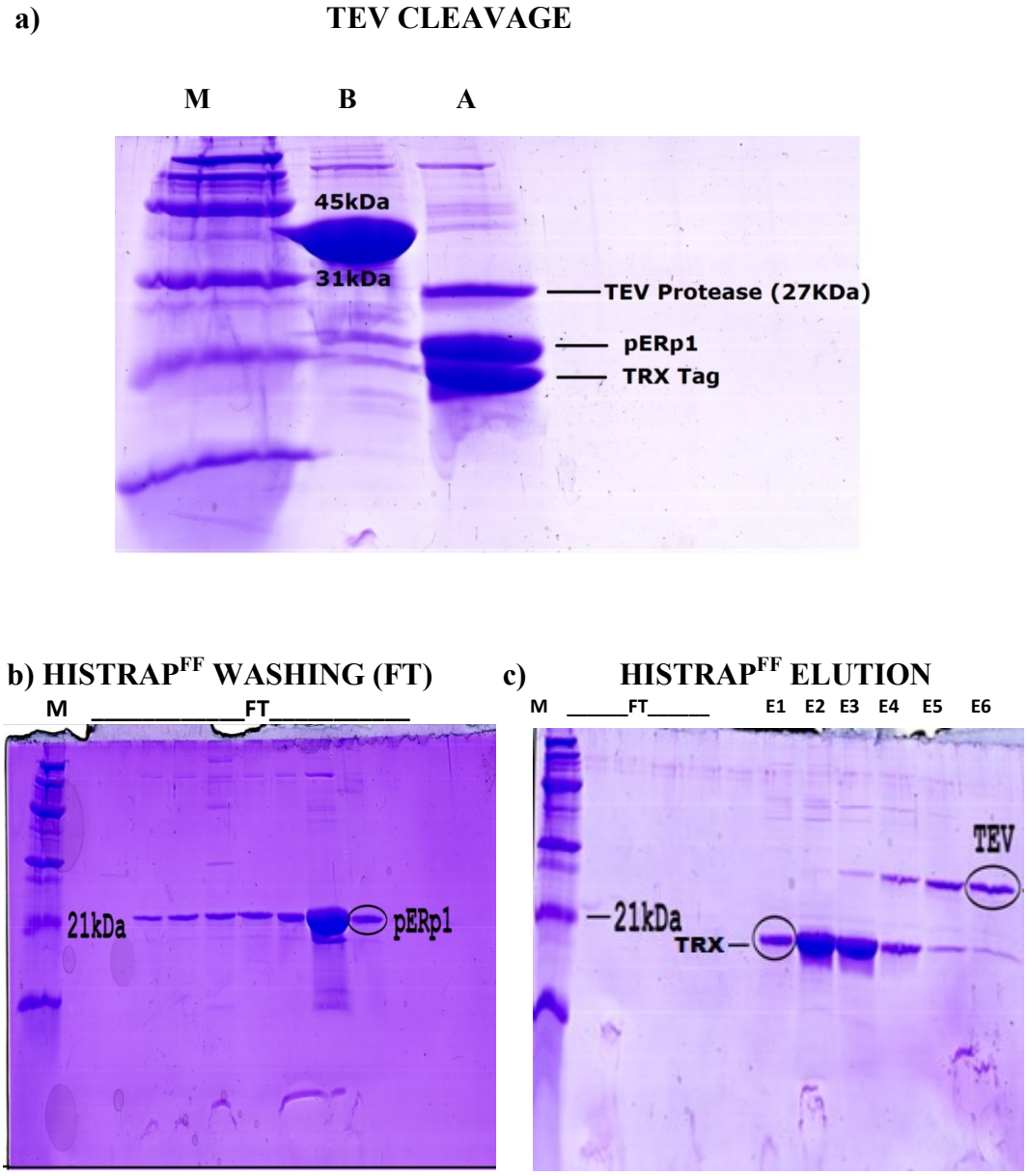

Figure 3.5 : SDS-PAGE analysis of the TEV cleavage and second HisTrap^{FF}. a) TEV cleavage reaction: After (A) and before (B) incubation with His-tag containing TEV protease. b) Washing phase fractions of HisTrap^{FF} : The pERp1 was collected from flowthrough since after TEV cleavage pERp1 does not include His-Tag. c) Fractions of the HisTrap^{FF} elution phase: Both TRX-Tag and TEV protease eluted from E1 to E6 fractions.

21 kDa pERp1 was seperated from TRX-Tag after 3 different purification steps were oparated by HisTrap^{FF}, Resource Q^{TM} and HiLoad Superdex 75 PG, respectively. After the cleavage reaction, both used TEV protease and TRX-Tag were polished off by additional process of HisTrap^{FF} chromatography, and pERp1 was collected from flowthrough whereas the used TEV protease and TRX-tag was eluted by immidazole containing Tris Buffer B.

3.4 Ubi-Grp94-Ubi Construct has slightly decreased K_{cat}

The K_{cat} values of both proteins were determined by using a coupled ATPase assay. The mean K_{cat} value for wt Grp94 was around 0.037 min^{-1} and Ubi-Grp94-Ubi exerts its ATPase activity as much as wt Grp94 does, with slight decrease, 0.034 min^{-1} at 30^0C. Standart devition collected from 3 independent measurements for both protein is in acceptable range.

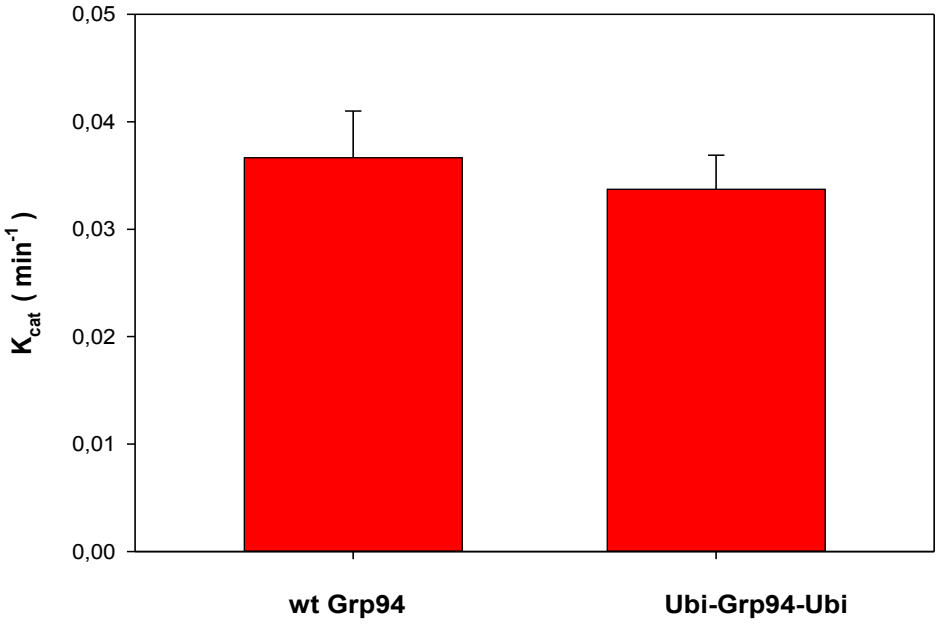

Figure 3.6 : K_{cat} values of wt Grp94 and Ubi-Grp94-Ubi constructs at 30 ^{0}C. The results are the mean of three measurements. The error bars indicate the standard deviations and red bars convey mean of K_{cat} collected from 3 independent measurements.

To determine a Michaelis Menten constant, K_m correspond to the substrate concentration by which the reaction rate is half of V_{max}, steady state kinetics examined with diffent concentrations of ATP at 37 ^{0}C. The plot was fit by using Michaelis Menten regression equation with the output of high r square. Interestingly, K_m is calculated as 185 µM which strikingly differs the value of wt Grp94 estimated in Frey's article, 92 µM (Frey et al., 2007). Additionaly, V_{max} of Ubi-Grp94-Ubi at 37 ^{0}C is calculated as '0.0479 min^{-1}' according to Michelis Menten equation. It can be interpreted as that ubiquitin tag influences affinity of ATP to Grp94. This might be resulted from disruption of binding pocket positioned in N-terminal domain by ubiquitin tag.

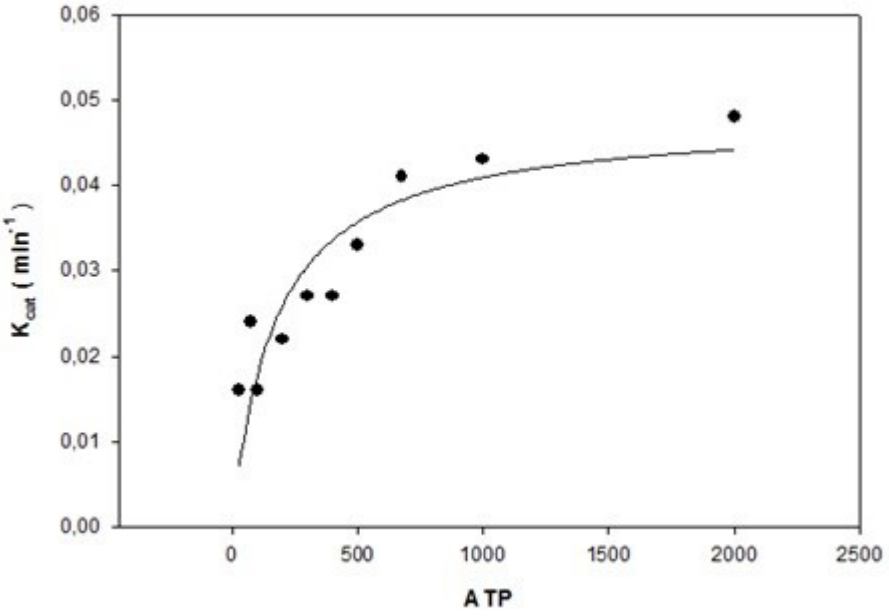

Figure 3.7 : K_m calculation of Ubi-Grp94-Ubi construct at 37 ^{0}C: The K_{cat} values in respect of different concentration of ATP are depicted as black dots in plot and fit by Michaelis Menten equation, are the mean of three measurements. According to the plot, K_m of Ubi-Grp94-Ubi is calculated as 185 μM.

3.5 pERp1/MZB1 stimulates ATPase Activity of the Constructs

ATPase assay of Grp94 and Ubi-Grp94-Ubi were conducted with the potential Grp94 co-chaperone pERp1/MZB1. Significant change in K_{cat} was observed, approximately 2 fold increase for each construct in the presence of equalar molar of pERp1 (pERp1 conducted wt Grp94 is about 0.081 min^{-1} and 0.079 min^{-1}). Ubi-Grp94-Ubi It should be noted that, first phase of $NADH^+$ decrease correspond to first 10 minutes is taken into account while the raw data was being processed since overall graph seems an exponential decrease plot rather than linear. It may caused from increased dissociation constant of pERp1-Grp94 complex once the nucleotide was introduced to the buffer. In other words, in the absence ATP, pERp1-Grp94 binding constant is possibly higher than that of in the presence of ATP and nucleotide shifts the equlibrium towards to dissociation. Supporting this, previously, it has been reported by a co-immunoprecipitation experiments that MZB1-Grp94 interaction is strongly regulated by nucleotide and ATP prevents binding of pERp1 (Rosenbaum et al., 2014).

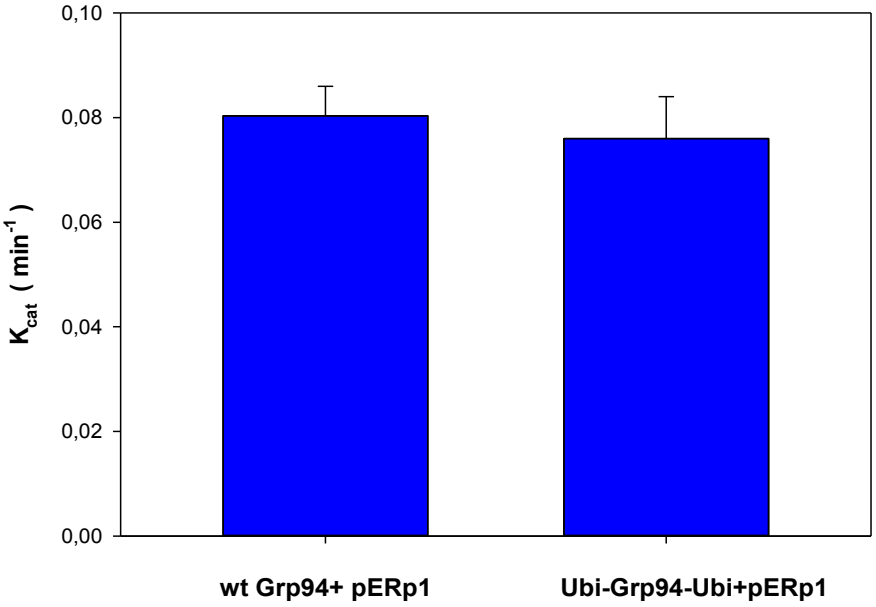

Figure 3.8 : K_{cat} values of wt Grp94 and Ubi-Grp94-Ubi proteins in the presence of pERp1/MZB1 (Grp94/Ubi-Grp94-Ubi:pERp1, 1:1 molar ratio) at 30 ^{0}C . The results are the mean of three measurements. The error bars indicate the standard deviations.

Half maximal effective concentration (EC_{50}) was evaluated as 28 μM with V_{max} as to be 19,3 fold of K_{cat} by titration of pERp1 into ATPase activity of Ubi-Grp94-Ubi.

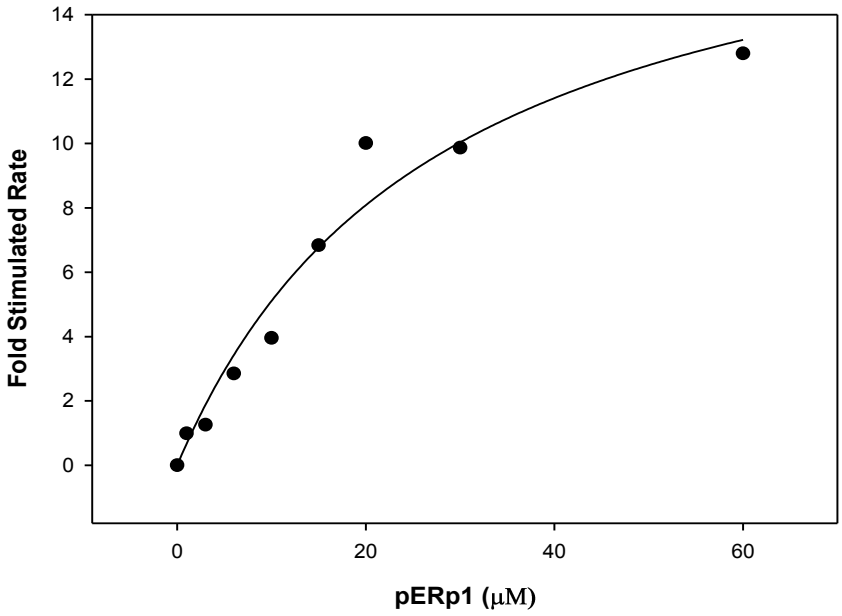

Figure 3.9 : Calculation of EC_{50} by titration of pERp1 to 3 μM Ubi-Grp94-Ubi at 30 ^{0}C. The results are the mean of three measurements and data are fit by single exponantial equation. EC_{50} was evaluated as 28 μM with V_{max}= 19,3 fold of the evaluated K_{cat}.

3.6 CD Measurements of Grp94 Construct

Secondary structure characterizations of both wt Grp94 and Ubi-Grp94-Ubi were analysed by using circular dichroism spectroscopy. CD scans were far UV and signals gained from both construct differ significantly. CD scan of the wt Grp94 has two minimals corresponding to 208 nm and 222 nm whereas that of Ubi-Grp94-Ubi includes one corresponding to 222 nm.

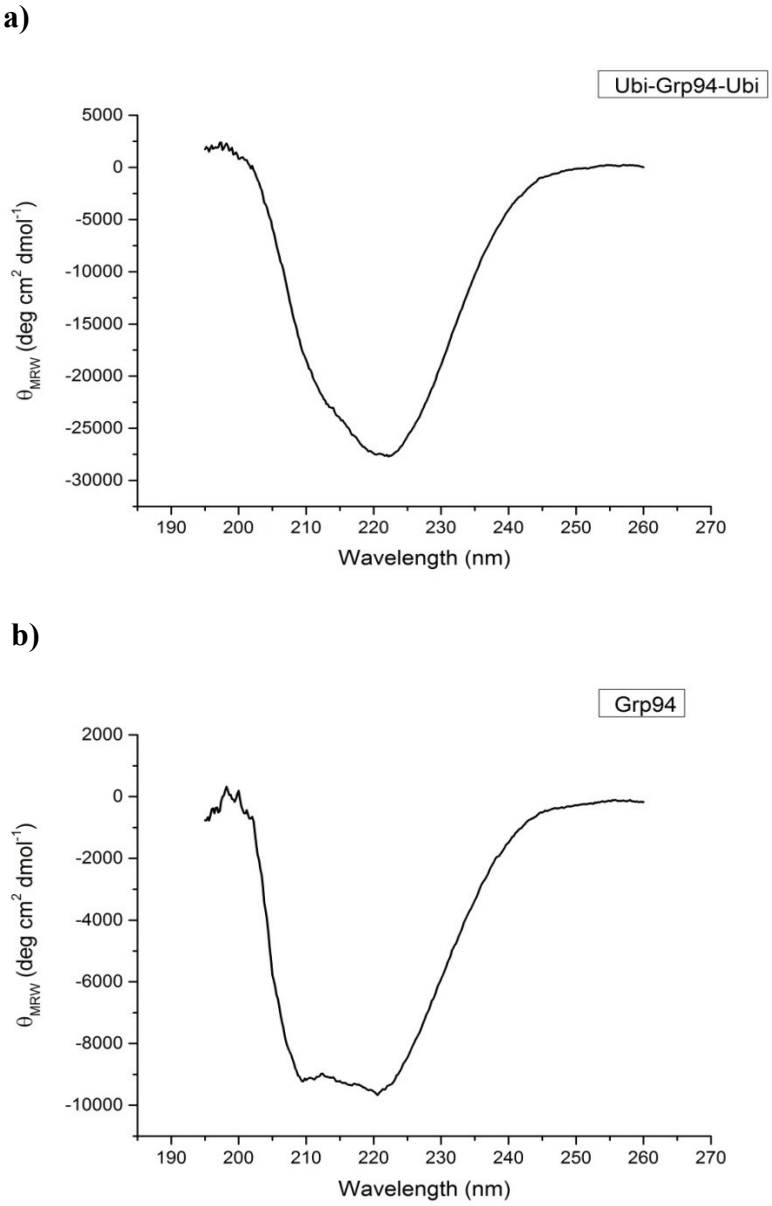

Figure 3.10 : Far UV CD measurements of Ubi-Grp94-Ubi and wt Grp94.

3.7 pERp1/MZB1 stimulates Citrate Synthase Aggregation

Together with activation of folded proteins, Hsp90 family interacts many cellular proteins in stress conditions such as high temperature in order to protect them to be misfolded or aggregated, which may result in toxicity for cell. Here, aggregation assay was performed by using a model substrate, 'Citrate Synthase (CS)' and the aggregation states have been monitored at 360 nm, 43 ^{0}C for each experiment, as described before with slight changes (Buchner et al., 1991).

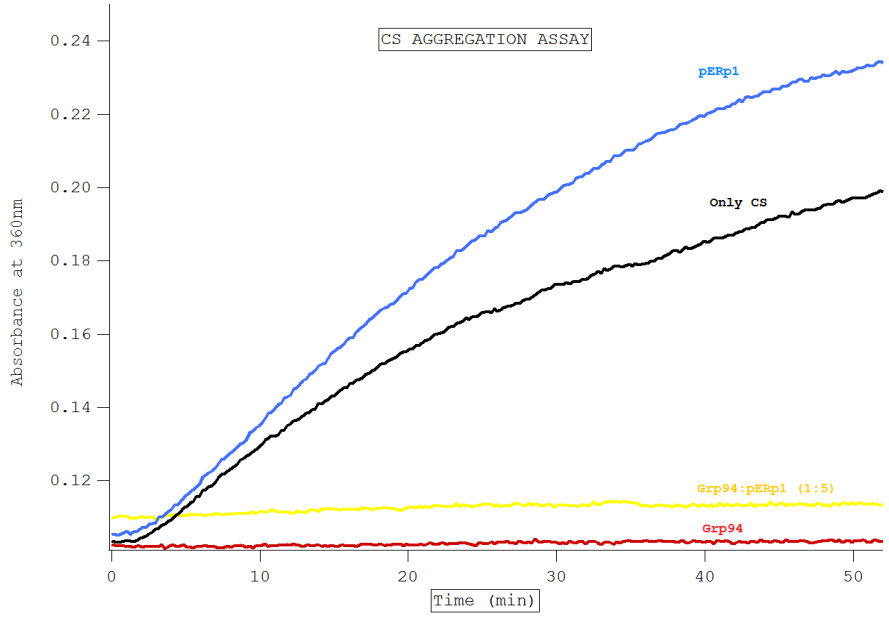

Figure 3.11 : Citrate synthase aggregation assay with different components and their combination: 0. 3 µM CS was used for each experiment in 40 mM HEPES Buffer at pH 7.5. The buffer was conducted independently to 1 µM Ubi-Grp94-Ubi (referred as to Grp94, red line), 5 µM pERp1 (blue) and combination of Ubi-Grp94-Ubi:pERp1 mix (yellow) in 1:5 molar ratio and prewarmed. Later CS was added before collecting data. The graph was plotted in two dimension, time (min) and absorbance at 360 nm. 'Only pERp1' exerts the highest aggregation progression, significantly higher than 'only CS' (black line). Grp94:pERp1 (1:5, yellow line) combination has no visible difference with only Ubi-Grp94-Ubi in CS aggregation measurements.

The experiments were operated in the presence of only Ubi-Grp94-Ubi, only pERp1 and both of protein, independently. Additionaly, the aggregation progress has been monitored in the presence of only citrate synthase as control. Interestingly, pERp1 conducted citrate synthase shows significantly stimulated aggregation whereas Ubi-Grp94-Ubi expectedly, supressed the aggregation progression.

3.8 Analytical Gel Filtration Assay

Early on, binding of pERp1 to Grp94 has been shown with co-IP experiments (Rosenbaum et al., 2014). Here, it was aimed to reveal the interaction by another technique, analytical gel filtration which would be validation of pre-identified pERp1-Grp94 complex. Gel filtration column in line with HPLC system is versatile and practical tool to detect protein-protein interaction including oligomerization states of certain proteins. In our experiments, respective proteins were conducted onto Superdex 200 10/300 GL, which 3 different conditions priorly were applied independently.

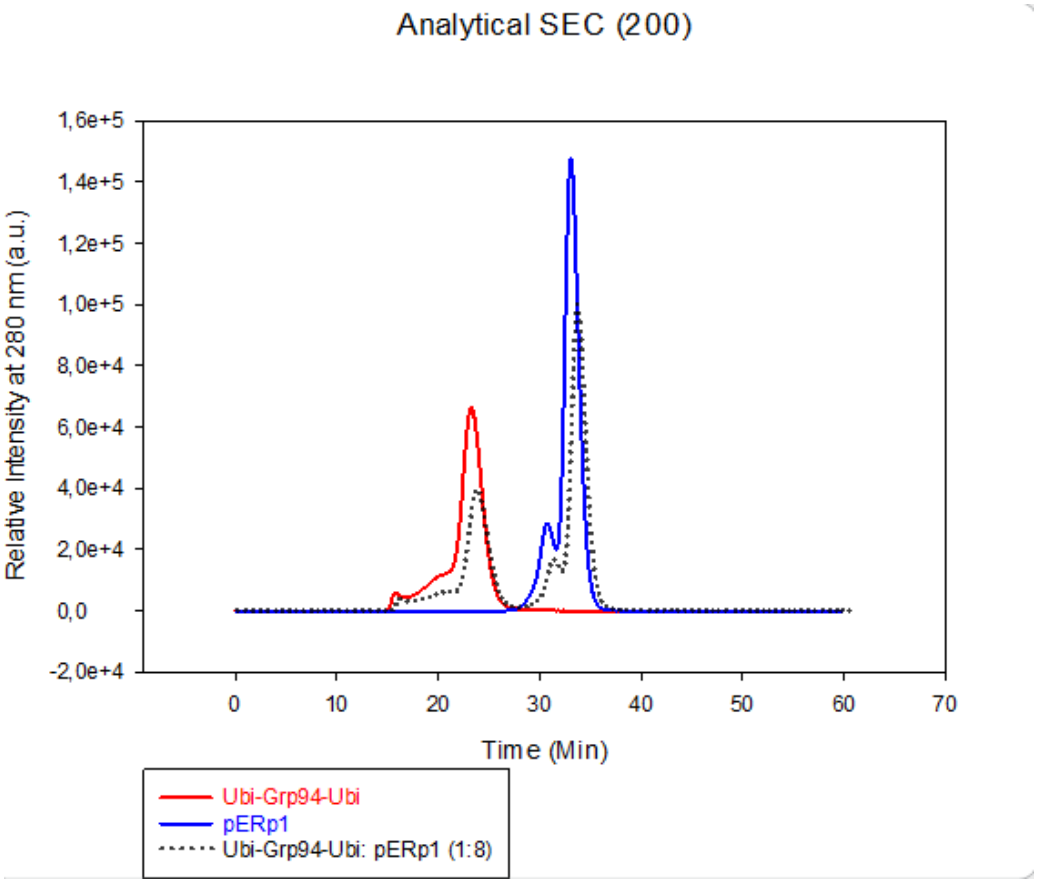

Figure 3.12 : Analytical size exclusion chromatograms of individual proteins Ubi-Grp94-Ubi, pERp1 and their combination.

Hereby, pERp1 and Ubi-Grp94-Ubi complex has not been shown by the analytical size exclusion chromatography (Figure 3.12). However, interestingly, a slight shoulder peak before main peak of pERp1, correspond to higher molecular weight than that of pERp1 has been observed on pERp1 chromatograph. This might be caused from dimeric form of pERp1.

4. DISCUSSION

The molecular chaperone Hsp90 is an essential eukaryotic protein which assists the final maturation of a set of client proteins. Unlike other chaperone families, the clients of Hsp90 have no defined motif that mediates interaction with the chaperone and interestingly, comprise diverse classes of proteins which are structurally unrelated. Hsp90 functions in an ATP-dependent fashion and undergoes conformational changes in which the states are energetically similar (Röhl et al., 2013). In the apo-form, Hsp90 adopts an open conformation whereas ATP binding induces a closed conformation. ATP binding leads to N- domain dimerization and it is followed by a contact of the M domain with the nucleotide- binding pocket of N domain (Ali et al., 2006). These conformational changes result in ATP hydrolysis with close proximity of the putative catalytic residue in M domain to the ATP in nucleotide binding pocket. The ADP-bound Hsp90 shows a highly compact state distinct from the closed AMP-PNP-bound state (Huai et al., 2005; Shiau et al., 2006). It should be noted that due to highly dynamic nature of Hsp90, nucleotide binding to Hsp90 slightly shifts the conformational equilibrium towards a closed state rather than dictating a certain conformation (Southworth et al., 2008; Krukenberg et al., 2009; Mickler et al., 2009). However, an EM study has demonstrated that all three conformations are conserved among cytosolic yeast, human and prokaryotic Hsp90s (Southworth et al., 2008). In this study, both Hsc82 from yeast and human Hsp90α were shown to adopt a closed state upon addition of a non-hydrolyzable ATP analogue, AMP-PNP and a more compact state by incubation with ADP. It is noteworthy that Grp94 resembles human Hsp90 referred as to 'Hsp90α' in magnitude of shift upon addition of ATP, which is less than that of Hsp82, its yeast cytosolic counterpart (Southworth et al., 2008).

Hsp90 is not alone to deal with diverse clients, but cooperates with a set of co-chaperone, which serve as client recruiters or function in remodelling of Hsp90 itself (Röhl et al., 2013). In the course of evolution, particularly for eukaryotes, the coordination with a set of accessory proteins is an expected adaptation of Hsp90 in

order to function as a chaperone interacting with structurally unrelated substrates. The diversity in co-chaperones allows Hsp90 interaction with specific clients, the stabilization of a certain conformation and the maturation of substrates or the recruitment of clients from Hsp70 (Lee et al., 2012; Schmid et al., 2012; Southworth et al., 2011; Roe et al., 2004). Therefore, the nature of the synergism between Hsp90 and its co-chaperones is at the center of current studies to elucidate the mechanistic, dynamic and functional properties of Hsp90. Here, in the context of this thesis, initial steps have been taken to elicit whether the endoplasmic reticulum paralog of Hsp90, Grp94 differs from its counterparts in terms of its ATPase kinetics. In the first part of the work, the ATPase activity of wt Grp94 and an N- and C-terminally ubiquitin-tagged Grp94 construct were determined and compared with each other. The K_{cat} value of wt Grp94 was determined 0.037 min^{-1} at 30 ^{0}C. Similarly, Ubi-Grp94-Ubi exerts 0.034 min^{-1}, slightly decreased compared to wt Grp94. One must be point out that Grp94 had long been conceived to have no intrinsic ATPase activity until a structural and a kinetic study independently demonstrated this (Dollins et al., 2007; Frey et al., 2007). Since the crystal structure of AMP-PNP-bound Grp94 revealed that the conserved catalytic residue R448 is far from the nucleotide binding pocket, it had been hypothesised that ATP hydrolysis is driven by either an unidentified co-chaperone or a client, but not the conformational change following ATP binding in cytoplasmic Hsp90. Importantly the two studies presented substantially different K_{cat} values, approximately 0.36 min^{-1} in Frey's study compared to a K_{cat} of 0.02 min^{-1} in Dollins' article which is more likely in line with our measurement. It should be considered that differences in the extent to which Grp94 was purified in the different studies might have led to deviations in the ATPase rate result in two different K_{cat} values. One may bear in mind that one or more *E. coli* protein contaminants present in purified Grp94 in Frey's study might have acted as accessory protein that influences the ATPase rate. This speculation is important, as mentioned above ATP binding itself might not be able to drive Grp94 N-terminal dimerization between protomers. Because it is known that *E. coli* proteome contains a set of immunoglobulin folding proteins (Bodelon et al., 2012) and an unidentified accessory contaminating native protein of host cell might interfere with the ATPase activity. Another reason behind this conflict between ATPase rates of these two different papers might have resulted from the N-terminal His-tag used in the Dollins paper, which may interrupt the ATPase cycle or binding of NECA.

However, the Dollins paper is in line with the data in this thesis, where not N-terminal His-tag was present and the Ubi-Grp94-Ubi construct exerts similar ATPase activity compared to wt Grp94. Therefore, rather than introduced tag into the Grp94, purification level must be the primary suspicious in deviation between our data and Frey's result.

In the second part of this work, the ATPase activity assay was conducted in combination with the potential Grp94 co-chaperone MZB1 which is also known as pERp1. pERp1 first has been identified by two independent studies. It is implicated in B cell differentiation, IgM biosynthesis and secretion (Shimizu et al., 2008; Anken et al., 2009). The question if Grp94 has any co-chaperones has not yet been clarified but there are some indications that Grp94 co-chaperones exist. A recent study has revealed that pERp1 knock-down in mouse leads to an impairment in antibody secretion and B-cell differentiation. The same study also stated that under ER stress conditions, pERp1 is required for the interaction of Grp94 with the immunoglobulin m heavy chain (Rosenbaum et al., 2014). Additionally, an earlier study pointed out that CNPY3 might be a presumptive Grp94 co-chaperone that is required for Toll-like biosynthesis (Liu et al., 2010). Interestingly, pERp1 and CNPY3 share homology and their interaction with Grp94 is nucleotide sensitive (Rosenbaum et al., 2014). Supporting this idea, CNPY3 study reported that mutation of a putative catalytic residue of Grp94, E103A resulted in loss of interaction significantly (Liu et al., 2010). A co-chaperone driven conformational shift of Grp94 has not been reported yet.

In our study, pERp1 addition causes a significant increase with two fold over the basal ATPase activity whereas an earlier study showed no impact of pERp1 on the ATPase activity of wt Grp94 (Rosenbaum et al., 2014). In this paper unlike in this thesis, geldanamycin was used as ATPase inhibitor to assess the background ATPase activity (i.e., the ATPase activity of contaminant proteins). One reason that my results differ from the previous study might thus be that geldanamycin is not as effective as NECA the specific inhibitor of Grp94, which was used in my thesis. The affinity or binding kinetics of the two inhibitors may differ from each other in the presence of pERp1 and we have no insight yet on the 3-D architecture of the pERp1-Grp94 interaction. Concerning this thesis, it must be pointed out that the initial 10 minutes is taken into account to calculate K_{cat} values in titration of pERp1. The

reason behind to prefer the first minutes in calculation is that the NADH oxidation pattern monitored during assay was more likely a single exponential decrease rather than linear. Linear plot is gradually turn into single exponential curve with increasing pERp1 concentration, is presumably consequence of pre-identified nucleotide regulated binding (Rosenbaum et al., 2014).

Regarding affinity of pERp1 and Grp94 interaction, one may bear in mind that our EC_{50} can be expected to be in good line with the dissociation constant which would be obtained from either ITC or CD. Surely, ATP has been shown to regulate binding; it must increase K_d and similarly, our raw ATPase activity data by time fits single exponential equation can be interpreted as effect of increasing binding constant between pERp1 and Grp94 upon addition of ATP. Therefore, EC_{50} must be higher than any K_d value which can be calculated by different approach in the absence of ATP, but rather low than that of in the presence of ATP.

Even though, it seems to be early to set a scenario concerning pERp1 regulated ATPase activity of Gpr94, pERp1 conducted steady state kinetic data shows significant increase in activity, can be clue of conformational re-arrangements which makes ATP hydrolysis favourable. It may be caused from relatively close proximity of R448, putative catalytic residue which is positioned in M domain upon interaction with pERp1. From different aspect, pERp1- bound Grp94 might be adopted to an unique conformation which cause less energetic burden for transition to catalytically active, N-terminally dimerized conformation by disturbing acquired twisted V conformation. Presumably, pERp1 navigates Grp94 to adopt conformationally more favourable state to hydrolyse ATP, before loading of nucleotide binding pocket with ATP. However, to clarify the structural basis of increased ATPase activity we need to refer structural techniques such as co-crystallization or NMR. Morever, ATP binding kinetics of pERp1-Grp94 should be calculated to reveal if the increased ATPase activity is resulted from higher affinity to ATP. However, this scenario seems less possible since Grp94 has relatively stronger binding affinity to ATP compared to other Hsp90s (Frey et al., 2007). Intriguingly, what might be the physiological relevance of the stimulated ATPase activity in immunoglobin maturation? Is pERp1 creating only an interaction platform for immunoglobin and if exists, in which aspects it regulates ATPase activity to demand its maturation? How the domain organisation re-arranged by pERp1 in respect to orientation at interfaces

between N-M and M-C? These are main questions which must be addressed as future aspect.

It has been earlier stated that pERp1 may be an unique chaperone for IgM monomers since pERp1 is still capable of binding to the monomers in the presence of DTT highlighting the binding does not primarily depends on cysteine cross-links (Anken et al., 2009). In our study, CS aggregation assay is operated to show chaperone activity of Grp94 and any possible effect of pERp1 on progression of the thermal aggregation. Interestingly, pERp1 remarkably stimulated to CS aggregation in our study. This may be caused from oxidoreductase activity of pERp1, leading CS to be more prone to be aggregated due to reduction of native disulfide bonds. Scrambled species with non-native disulfide bonds might be propagated and consequently contributed to thermal aggregation. Another possibility is that it might be an artefact which is resulted from high molar usage of pERp1 (5 μM).

In conclusion, our data indicate that pERp1 impacts the ATPase activity and exhibits moderate binding constant regarding the interaction with Grp94. However, the mechanism of pERp1 interaction with Grp94 is still in its infant phase. An intriguing question to be addressed in the future is whether the interaction of pERp1 affects the conformational equilibrium of Grp94 in solution. Dissecting a possible regulation of Grp94 by a potential co-chaperone would not only facilitate elucidating the gear of Grp94's molecular mechanism but also give first insights of immunoglobin maturation basis.

REFERENCES

Ali, M. M., Roe, S. M., Vaughan, C. K., Meyer, P., Panaretou, B., Piper, P. W., Prodromou, C., Pearl, L. H. (2006). Crystal structure of a Hsp90-nucleotide-p23/Sba1 closed chaperone complex. *Nature.* 440(7087), 1013-7.

Anfinsen, C. B. (1973). Principles that govern the folding of protein chains. *Science*. 181(4096), 223-30.

Ban, N., Nissen, P., Hansen, J., Moore, P. B., Steitz, T. A. (2000). The complete atomic structure of the large ribosomal subunit at 2.4 A resolution. *Science*. 289(5481), 905-20.

Bakthisaran, R., Tangirala, R., Rao, M. (2015). Small heat shock proteins: Role in cellular functions and pathology. *Biochim. Biophys. Acta.* 1854(4): 291-319.

Biswas, C., Ostrovsky, O., Makarewich, C. A., Wanderling, S., Gidalevitz, T., Argon, Y. (2007). The peptide binding activity of GRP94 is regulated by calcium. *Biochem. J.* 405 (2007), 233–241.

Bertelsen, E. B., Chang, L., Gestwicki, J. E., Zuiderweg, E. R. (2009). Solution conformation of wild-type *E. coli* Hsp70 (DnaK) chaperone complexed with ADP and substrate. *Proc. Natl. Acad. Sci*. 106(21): 8471-6.

Bodelón, G., Palomino, C., Fernández, L. Á. (2013). Immunoglobulin domains in *Escherichia coli* and other enterobacteria: from pathogenesis to applications in antibody technologies. *FEMS. Microbio. Rev.* 37(2), 204-50.

Buchner, J., Schmidt, M., Fuchs, M., Jaenicke, R., Rudolph, R., Schmid, F. X., Kiefhaber, T. (1991). GroE facilitates refolding of citrate synthase by suppressing aggregation. *Biochemistry*. 30(6): 1586-91.

Chang, H., Tang Y., Hayer-Hartl M., Hartl, F. U. (2007). SnapShot: Molecular Chaperones, Part I. *Cell*. 128, 212.

Deuerling, E., Bukau, B. (2004). Chaperone-assisted folding of newly synthesized proteins in the cytosol. *Crit. Rev. Biochem. Mol. Biol.* 39(5-6), 261-77.

Dollins, D. E., Warren, J. J., Immormino, R. M., Gewirth, D. T. (2007). Structures of GRP94- nucleotide complexes reveal mechanistic differences between the hsp90 chaperones. *Mol. Cell*. 28, 41–56.

Doyle, S. M., Genest, O., Wickner, S. (2013). Protein rescue from aggregates by powerful molecular chaperone machines. *Nat. Rev. Mol. Cell Biol.* 14(10): 617-29.

Doyle, S. M., Shorter, J., Zolkiewski, M., Hoskins, J. R., Lindquist, S., Wickner, S. (2007). Asymmetric deceleration of ClpB or Hsp104 ATPase activity unleashes protein-remodeling activity. *Nat. Struct. Mol. Biol.* 14(2): 114-22.

Doyle, S. M., Wickner, S. (2009). Hsp104 and ClpB: protein disaggregating machines. *Trends. Biochem. Sci.* 34(1): 40-8.

Eletto, D., Dersh, D., Argon, Y. (2010). GRP94 in ER quality control and stress responses. *Semin. Cell. Dev. Biol.* 21(5), 479–485.

Ellis, R. J., Minton, A. P. (2006). Protein aggregation in crowded environments. *Biol. Chem.* 387(5), 485-97.

Frey, S., Leskovar, A., Reinstein, J., Buchner, J. (2007). The ATPase cycle of the endoplasmic chaperone Grp94. *J. Biol. Chem.* 282(49), 35612-20.

Hartl, F. U., Hayer-Hartl, M. (2009). Converging concepts of protein folding in vitro and in vivo. *Nat. Struct. Mol. Biol.* 16(6), 574-81.

Hartl, F. U., Bracher, A., Hayer-Hartl, M. (2011). Molecular chaperones in protein folding and proteostasis. *Nature.* 475, 324–332.

Hessling, M., Richter, K., Buchner, J. (2009). Dissection of the ATP-induced conformational cycle of the molecular chaperone Hsp90. *Nat. Struct. Mol. Biol.* 16(3), 287-93.

Horwich, A. L., Fenton, W. A., Chapman, E., Farr, G. W. (2007). Two families of chaperonin: physiology and mechanism. *Annu. Rev. Cell. Dev. Biol.* 23: 115-45.

Huai, Q., Wang, H., Liu, Y., Kim, H. Y., Toft, D., Ke, H. (2005). Structures of the N-terminal and middle domais of *E. coli* Hsp90 and conformation changes upon ADP binding. *Structure*. 13, 579-590.

Immormino, R. M., Dollins, D. E., Shaffer, P. L., Soldano, K. L., Walker,M. A., Gewirth, D. T. (2004). Ligand-induced conformational shift in the N-terminal domain of GRP94, an Hsp90 chaperone. *J. Biol. Chem.* 279, 46162-46171.

Jeong, J. Y., Yim, H. S., Ryu, J. Y., Lee, H. S., Lee, J. H. (2012). One-step sequence and ligation-independent cloning as a rapid and versatile cloning method for functional genomics studies. *Appl. Environ. Microbiol.* 78, 5440–5443.

Johnson, J. L. (2012). Evolution and function of diverse Hsp90 homologs and cochaperone proteins. *Biochim. Biophys. Acta.* 1823(3), 607-13.

Karagöz, G. E., Rüdiger, S. G. (2015). Hsp90 interaction with clients. *Trends. Biochem. Sci.* 40(2), 117-25.

Katayama-Fujimura, Y., Gottesman, S., Maurizi, M. R. (1987). A multiple-component, ATP-dependent protease from *Escherichia coli*. *J. Biol. Chem.* 262(10): 4477-85.

Kerner, M. J., Naylor, D. J., Ishihama, Y., Maier, T., Chang, H. C., Stines, A. P., Georgopoulos, C., Frishman, D., Hayer-Hartl, M., Mann, M., Hartl, F. U. (2005). Proteome-wide analysis of chaperonin-dependent protein folding in *Escherichia coli*. *Cell.* 122(2): 209-20.

Kim, Y. E., Hipp, M. S., Bracher, A., Hayer-Hartl, M., Hartl, F. U. (2013). Molecular chaperone functions in protein folding and proteostasis. *Annu. Rev. Biochem.* 82: 323-55.

Kityk, R., Kopp, J., Sinning, I., Mayer, M. P. (2012). Structure and dynamics of the ATP-bound open conformation of Hsp70 chaperones. *Mol. Cell.* 48(6): 863-74.

Krukenberg, K. A., Bottcher, U. M., Southworth, D. R., Agard, D. A. (2009). Grp94, the endoplasmic reticulum Hsp90, has a similar solution conformation to cytosolic Hsp90 in the absence of nucleotide. *Protein. Sci.* 18, 1815–1827.

Krukenberg, K. A, Southworth, D. R., Street, T. O., Agard, D. A. (2009). pH-dependent conformational changes in bacterial Hsp90 reveal a Grp94-like conformation at pH 6 that is highly active in suppression of citrate synthase aggregation. *J. Mol. Biol.* 390, 278–91.

Krukenberg, K. A., Street, T. O., Lavery, L. A., Agard, D. A. (2011). Conformational dynamics of the molecular chaperone Hsp90. *Q. Rev. Biophys.* 44(2), 229-55.

Lee, C. T., Graf, C., Mayer, F. J., Richter, S. M., Mayer, M. P. (2012). Dynamics of the regulation of Hsp90 by the co-chaperone Sti1. *EMBO. J.* 31, 1518–1528.

Lee, S., Sowa, M. E., Watanabe, Y., Singler, P. B, Chiu, W., Yoshida, M., Tsai F. T. (2003). The Structure of ClpB. A molecular chaperone that rescues proteins from an aggregated state. *Cell.* 115, 229-240.

Li, J., Soroka, J., Buchner, J. (2012). The Hsp90 chaperone machinery: conformational dynamics and regulation by co-chaperones. *Biochim. Biophys. Acta.* 1823(3), 624-35.

Liu, B., Yang, Y., Qiu, Z., Staron, M., Hong, F., Li, Y., Wu, S., Li, Y., Hao, B., Bona, R., Han, D., Li, Z. (2010). Folding of Toll-like receptors by the HSP90 paralogue gp96 requires a substrate-specific cochaperone. *Nat. Commun.* 1(6), 1–10.

Lu, J. L., Deutsch, C. (2005). Folding zones inside the ribosomal exit tunnel. *Nat. Struct. Mol. Biol.* 12, 1123–1129.

Macer, D., Koch, G. L. R. (1988). Identification of a set of calcium-binding protein in reticuloplasm, the luminal content of the endoplasmic reticulum. *J. Cell. Sci.* 91, 61–70.

Mayer, M. P. (2013). Hsp70 chaperone dynamics and molecular mechanism. *Trends. Biochem. Sci.* 38(10): 507-14.

McLaughlin, S. H, Ventouras, L., Lobbezoo B., Jackson, S. E. (2004). Independent ATPase activity of Hsp90 subunits creates a flexible assembly platform. *J. Mol. Biol.* 344(3): 813-26.

Melnick, J., Dul, J. L., Argon, Y. (1994). Sequential interaction of the chaperones BiP and GRP94 with immunoglobulin chains in the endoplasmic reticulum. *Nature.* 370, 373–375.

Mickler, M., Hessling, M., Ratzke, C., Buchner, J., Hugel, T. (2009). The large conformational changes of Hsp90 are only weakly coupled to ATP hydrolysis. *Nat. Struct. Mol. Biol.* 16(3), 281-6.

Mogk, A., Kummer, E., Bukau, B. (2015). Cooperation of Hsp70 and Hsp100 chaperone machines in protein disaggregation. *Front. Mol. Biosci.* 19; 2: 22.

Ortega, J., Lee, H. S., Maurizi, M. R., Steven, A. C. (2004). ClpA and ClpX ATPases bind simultaneously to opposite ends of ClpP peptidase to form active hybrid complexes. *J. Struct. Biol.* 146(1-2): 217-26.

Ostrovsky, O., Ahmed, N. T., Argon, Y. (2009). The chaperone activity of GRP94 towards of insulin-like growth factor II is necessary for the stress response to serum deprivation. *Mol. Biol. Cell.* 20, 1855–64.

Panaretou, B., Prodromou, C., Roe, S. M., O'Brien, R., Ladbury, J. E., Piper, P. W., Pearl, L. H. (1998). ATP binding and hydrolysis are essential to the function of the Hsp90 molecular chaperone in vivo. *EMBO. J.* 17(16), 4829-36.

Pearl, L. H., Prodromou, C. (2006). Structure and mechanism of the hsp90 molecular chaperone machinery. *Annu. Rev. Biochem.* 75, 271–294.

Pratt, W. B., Toft, D. O. (2003). Regulation of signaling protein function and trafficking by the hsp90/hsp70-based chaperone machinery. *Exp. Biol. Med.* 228(2), 111-33.

Randow, F., Seed, B. (2001). Endoplasmic reticulum chaperone gp96 is required for innate immunity but not cell viability. *Nat. Cell. Biol*. 3, 891–896.

Richter, K., Soroka, J., Skalniak, L., Leskovar, A., Hessling, M., Reinstein, J., Buchner, J. (2008). Conserved conformational changes in the ATPase cycle of human Hsp90. *J. Biol. Chem.* 283(26), 17757-65.

Roe, S. M., Ali, M. M., Meyer, P., Vaughan, C. K., Panaretou, B., Piper, P. W., Prodromou, C., Pearl, L. H. (2004) The mechanism of Hsp90 regulation by the protein kinase-specific cochaperone p50(cdc37). *Cell.* 116, 87–98**.**

Rosenbaum, M., Andreani, V., Kapoor, T., Herp, S., Flach, H., Duchniewicz, M., Grosschedl, R. (2014). MZB1 is a GRP94 cochaperone that enables proper immunoglobulin heavy chain biosynthesis upon ER stress. *Genes. Dev.* 8(11), 1165-78.

Rosenzweig, R., Moradi, S., Zarrine-Afsar, A., Glover, J. R., and Kay, L. E. (2013). Unraveling the mechanism of protein disaggregation through a ClpB- DnaK interaction. *Science.* 339, 1080–1083**.**

Röhl, A., Rohrberg, J., Buchner, J. (2013). The chaperone Hsp90: changing partners for demanding clients. *Trends. Biochem. Sci.* 38, 253 - 262.

Rüdiger, S., Germeroth, L., Schneider-Mergener J., Bukau, B. (1997). Substrate specificity of the DnaK chaperone determined by screening cellulose-bound peptide libraries. *EMBO. J.* 16(7): 1501-7.

Schmid, A. B., Lagleder, S., Gräwert, M. A., Röhl, A., Hagn, F., Wandinger, S. K., Cox, M. B., Demmer, O., Richter, K., Groll, M., Kessler, H., Buchner, J. (2012). The architecture of functional modules in the Hsp90 co-chaperone Sti1/Hop. *EMBO. J.* 31, 1506–1517.

Shaffer, A. L., Shelef, M., Iwakoshi, N. N., Lee, A. H., Qian, S. B., Zhao, H., Yu, X., Yang, L.,Tan, B. K., Rosenwald, A.,Hurt, E. M., Petroulakis, E., Sonenberg, N., Yewdell, J. W., Calame, K., Glimcher, L. H., Staudt, L. M. (2004). XBP1, downstream of Blimp-1, expands the secretory apparatus and other organelles, and increases protein synthesis in plasma cell differentiation. *Immunity.* 21, 81–93.

Shiau, A. K., Harris, S. F., Southworth, D. R., Agard, D. A. (2006). Structural analysis of *E. coli* Hsp90 reveals dramatic nucleotide-dependent conformational rearrangements. *Cell.* 127(2), 329-40.

Shimizu, Y., Meunier, L., Hendershot, L. M. (2009). pERp1 is significantly up-regulated during plasma cell differentiation and contributes to the oxidative folding of immunoglobulin. *Proc. Natl. Acad. Sci.* 106, 17013–17018**.**

Solit, D. B., Rosen, N. (2006). Hsp90: a novel target for cancer therapy. *Curr. Top. Med. Chem.* 6(11), 1205-14.

Southworth, D. R., Agard, D. A. (2008). Species-dependent ensembles of conserved conformational states define the Hsp90 chaperone ATPase cycle. *Mol. Cell.* 32, 631-640.

Southworth, D. R., Agard, D. A. (2011). Client-loading conformation of the Hsp90 molecular chaperone revealed in the cryo-EM structure of the human Hsp90:Hop complex. *Mol. Cell.* 42, 771–781.

Tang, Y., Chang, H., Hayer-Hartl M., Hartl, F. U. (2007). SnapShot: Molecular Chaperones, Part I. *Cell.* 128, 412.

Vabulas, R. M., Raychaudhuri, S., Hayer-Hartl, M., Hartl, F. U. (2010). Protein folding in the cytoplasm and the heat shock response. *Cold. Spring. Harb. Perspect. Biol.* 2(12), a004390.

van Anken, E., Romijn, E. P., Maggioni, C., Mezghrani, A., Sitia, R., Braakman, I., Heck, A. J. R. (2003). Sequential waves of functionally related proteins are expressed when B cells prepare for antibody secretion. *Immunity.* 18, 243–253.

van Anken, E., Pena, F., Hafkemeijer, N., Christis, C., Romijn, E. P., Grauschopf, U., Oorschot, V. M., Pertel, T., Engels, S., Ora, A. (2009). Efficient IgM assembly and secretion require the plasma cell induced endoplasmic reticulum protein pERp1. *Proc. Natl. Acad. Sci.* 106, 17019–17024.

Van, P. N., Peter, F., Soling, H. D. (1989). Four intracisternal calcium-binding glycoproteins from rat liver microsomes with high affinity for calcium. No indication for calsequestrin-like proteins in inositol 1,4,5-trisphosphate-sensitive calcium sequestering rat liver vesicles. *J. Biol. Chem.* 264, 17494–17501.

Vitadello, M., Penzo, D., Petronilli, V., Michieli, G., Gomirato, S., Menabo, R., Di Lisa, F., Gorza, L. (2003). Overexpression of the stress protein Grp94 reduces cardiomyocyte necrosis due to calcium overload and simulated ischemia. *FASEB. J.* 17, 923–925.

Wanderling, S., Simen, B. B., Ostrovsky, O., Ahmed, N. T., Vogen, S., Gidalevitz, T. (2007). GRP94 is essential for mesoderm induction and muscle development because it regulates IGF secretion. *Mol. Biol. Cell.* 18, 3764–75.

Wandinger, S. K., Richter, K., Buchner, J. (2008). The Hsp90 chaperone machinery. *J. Biol. Chem.* 283(27), 18473-7.

Walter, S., Buchner, J. (2002). Molecular chaperones--cellular machines for protein folding. *Angew. Chem. Int. Ed. Engl.* 41(7): 1098-113.

Wiest, D. L., Burkhardt, J. K., Hester, S., Hortsch, M., Meyer, D. I., Argon, Y. (1990). Membrane biogenesis during B cell differentiation: Most endoplasmic reticulum proteins are expressed coordinately. *J. Cell. Biol.* 110, 1501–1511.

Yang, Y., Liu, B., Dai, J., Srivastava, P. K., Zammit, D. J., Lefrancois, L., Li, Z. (2007). Heat shock protein gp96 is a master chaperone for toll-like receptors and is important in the innate function of macrophages. *Immunity*. 26, 215–226.

Young, J. C, Moarefi, I., Hartl, F. U. (2001). Hsp90: a specialized but essential protein-folding tool. *J. Cell Biol.* 154(2), 267–274.

Zimmerman, S. B., Trach, S. O. (1991). Estimation of macromolecule concentrations and excluded volume effects for the cytoplasm of *Escherichia coli*. *J. Mol. Biol.* 222(3), 599-620**.**

Zimmerman, S. B., Minton, A. P. (1993). Macromolecular crowding: biochemical, biophysical, and physiological consequences. *Annu. Rev. Biophys. Biomol. Struct.* 22, 27-65.

APPENDICES

APPENDIX A : Laboratory equipments

APPENDIX B : Chemicals and enzymes

APPENDIX C : Buffers and solutions

APPENDIX A

Äkta FPLC machine	Amersham, Uppsala, Sweden
Amicon Ultra 4 mL centrifugal filter	Merck, Darmstadt, Germany
Amicon Ultra 15 mL centrifugal filter	Merck, Darmstadt, Germany
Avanti J 25 centrifuge	Beckman, Wien, Austria
Balance BP 121 S S	Sartorius, Göttingen, Germany
Balance BL 310	Sartorius, Göttingen, Germany
Cell disruption machine Basic Z	Constant Systems, Warwick, England
Certomat S Shaker	Braun Biotech, Melsungen, Germany
DEAE Sephacel	GE Healthcare, Freiburg, Germany
Dialysis membrane	Spectrum, Houston, USA
Eppendorf 5415 C centrifuge	Eppendorf, Hamburg, Germany
Eppendorf thermomixer	Eppendorf, Hamburg, Germany
GradiFrac system	Amersham, Uppsala, Sweden
Hoefer Mighty Small II gel electrophoresis	Amersham, Uppsala, Sweden
HPLC PU-1850, UV-1575	Jasco, Gross-Umstadt, Germany
Ice machine	Ziegra, Isernhagen, Germany
Jasco J715	Jasco, Groß-Umstadt, Germany
LKB GPS 200/400 voltage source	Amersham, Uppsala, Sweden
Magnetic Stirrers MR 2000	Heidolph, Kelheim, Germany
Ni-NTA HisTrap^{FF}	GE Healthcare, Freiburg, Germany
pH-meter	WTW, Weilheim, Germany
Primus Thermocycler	MWG, Ebersberg, Germany
Resource Q 6 ml	GE Healthcare, Freiburg, Germany
Sonifier B-12	Branson, Danbury, USA
HiLoad Superdex 75 PG	GE Healthcare, Freiburg, Germany
HiLoad Superdex 200 PG	GE Healthcare, Freiburg, Germany

Superdex 200 PG 10/300 GL	GE Healthcare, Freiburg, Germany
Varian Cary 50 UV-Vis spectrophotometer	Varian, Palo Alto, USA
Varioklav steam autoclave EP-Z	H+P, Oberschleißheim, Germany

APPENDIX B

Acrylamide (38:2% Bisacrylamide)	Roth, Karlsruhe, Germany
Adenosin-5´-triphosphate disodium salt	Roche, Mannheim, Germany
Agarose powder	Roche, Mannheim, Germany
Ammoniumperoxodisulfate (APS)	Roche, Mannheim, Germany
Ampicillin	Roth, Karlsruhe, Germany
Alexa Fluor 488 maleimide	Invitrogen, Carlsbad, USA
Bromphenol blue S	Serva, Heidelberg, Germany
Calcium chloride	Merck, Darmstadt, Germany
Coomassie Brilliant Blue G-250	Serva, Heidelberg, Germany
Dithiothreitol (DTT)	Roth, Karlsruhe, Germany
Ethanol	Roth, Karlsruhe, Germany
Ethidiumbromide	Sigma, St. Louis, USA
HEPES	Sigma, St. Louis, USA
Hind III HF	New England Biolabs, Germany
Kanamycin	Roth, Karlsruhe, Germany
Lactate dehydrogenase (LDH)	Roche, Mannheim, Germany
Magnesium chloride hexahydrate	Merck, Darmstadt, Germany
Nicotinamide adenine dinucleotide	Roche, Mannheim, Germany
N,N,N',N'-Tetramethylethylendiamin	Roth, Karlsruhe, Germany
Imidazole	Sigma, St. Louis, USA
Isopropylβ-D-1-thiogalactopyranoside	Merck, Darmstadt, Germany
Pfu DNA polymerase	Promega, Madison, USA
Phosphoenolpyruvate (PEP)	Roche, Mannheim, Germany
Potassium chloride	Merck, Darmstadt, Germany
Protease inhibitor mix G	Serva, Heidelberg, Germany
Protease inhibitor mix HP	Serva, Heidelberg, Germany

Pyruvate kinase (PK)	Roche, Mannheim, Germany
SacI HF	New England Biolabs, Germany
Sodium chloride	Merck, Darmstadt, Germany
Sodium dihydrogen phosphate dehydrate	Merck, Darmstadt, Germany
Sodiumdodecylsulfate (SDS)	Roth, Karlsruhe, Germany
Tris-(hydroxymethyl)-aminomethan (TRIS)	ICN, Irvine, USA
5'-N-ethylcarboxamidoadenosine	Sigma, St. Louis, USA

APPENDIX C

15% Separation gel :	3.75 mL 40% Acrylamide (Acryl./Bisacryl. 38:2)
	2.50 mL 4x SDS-Buffer (0.8% SDS, 1.5 M Tris, pH 8.8)
	3.75 mL dH2O
10% Separation gel :	2.50 mL 40% Acrylamide (Acryl./Bisacryl. 38:2)
	2.50 mL 4x SDS-Buffer (0.8% SDS, 1.5 M Tris, pH 8.8)
	5.00 mL dH2O
5% Stacking gel :	0.625 mL 40% Acrylamide (Acryl./Bisacryl. 38:2)
	2.50 mL 2x SDS-Buffer (0.4% SDS, 0.3 M Tris, pH 6.8)
	1.875 mL dH2O

TAE (50x) : 2 M Tris/acetate pH 8.0, 50 mM EDTA pH 8.0

SDS running buffer (10x) : 250 mM Tris/HCl pH 6.8 2 M Glycine 1% (w/v) SDS

SDS running buffer (10x) : 250 mM Tris/HCl pH 6.8 2 M Glycine 1% (w/v) SDS

SDS sample buffer (5x) : 312.5 mM Tris/HCl pH 6.8,10% (w/v) SDS 50% (v/v) Glycerol 2.5% (v/v) β-mercaptoethanol 0.05% (w/v) bromphenolblue

Fairbanks A : 2.5 g Coomassie Brilliant Blue R-250, 250 mL Ethanol, 80 mL Acetic acid adjusted to 1 L with H_2O

Fairbanks D : 250 mL Ethanol, 80 mL Acetic acid, 670 ml H_2O

Buffer A : 40 mM HEPES, 50 mM KCl, and 10 mM $CaCl_2$, pH 7.5, 1 mM DTT.

Buffer B : 40 mM HEPES, 0.5 M KCl, and 10 mM $CaCl_2$, pH 7.5, 1 mM DTT.

Buffer C : 40 mM HEPES, 0.5 M KCl, and 5 mM $MgCl_2$, pH 7.5, 1 mM DTT.

Phosphate Buffer A : 20 mM NaH_2PO_4, 500 mM NaCl, 20 mM imidazole, pH 7.5.

Phosphate Buffer B : 20 mM NaH_2PO_4, 500 mM NaCl, 500 mM imidazole, pH 7.5.

Tris Buffer A : 50 mM TRIS, 50 mM NaCl, pH 7.5, 0.5 mM DTT.

Tris Buffer B : 50 mM TRIS, 500 mM NaCl, pH 7.5, 0.5 mM DTT.

CURRICULUM VITAE

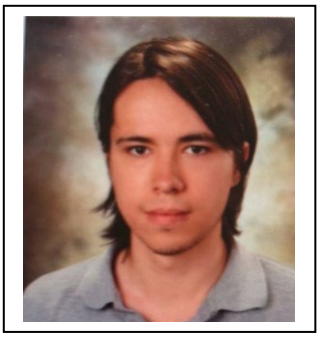

Name Surname	**: Mustafa Barbaros DÜZGÜN**
Place and Date of Birth	**: Çanakkale/ TURKEY, 24.05.1989**
E-Mail	**:** barbarosduzgun@gmail.com
B.Sc.	**:** Istanbul Technical University
M.Sc.	**:** Istanbul Technical University

Professional Experience and Rewards :

- 2010 (3 months) Summer Internship at Senatoryum Hospital: Immunostaining techniques and microscopy of lung tissue have been operated with the assistance of the section officials.
- 2011-2013 Student Researcher at Dinler Lab: The project was based on mutational study regarding nucleotide bining domain of *E.coli* Hsp70, DnaK, by which allosteric mechanism playing central role in interplay between the two domains was aimed to be elucidated with residual basis.
- 2014 (4 months) Student Researcher at Karagüler Lab: The study focused on efficient expression and purification of *E.coli* Aquaporin protein to be analyzed and utilized in developing a water purification system within aspects of biotechnology.
- 2014-2015 (1 year) Erasmus Exchange Programme Scholarship: This master thesis has been performed by aid of financial support provided in the context of Erasmus Exchange Programme.
- 2014-2015 (9 month) Master Thesis Project at Buchner Lab
- 2014-2015 (3 month) Student Assistantship (Studentische Hilfskraft) at Weinkauf Lab: The main purpose of the participated study was disclosing structural basis of oligomeric behaviour of alpha-ctystallin which is a member of small heat-shock proteins. The basics of single particle analysis of EM techniques have been partly acquired during the part-time job.